

Feasibility research: Design of a mini-Tension Leg Platform foundation for a 6MW Wind Turbine

Part of MSc-Internship at MECAL B.V.



Ramon Mertens
Internship_feasibility_research_mini_TLP
07/01/2015

Commissioned by:
MECAL Wind Turbine Design B.V.
Eyal Taub
Capitool 15,
7500 AG, Enschede
The Netherlands



Title document:

Feasibility research: Design of a mini-Tension Leg Platform foundation for a 6MW Wind Turbine

Date:	07/01/2015
Written by:	Ramon Mertens, MECAL WTD
Checked by:	Eyal Taub, MECAL WTD
Commissioned by:	Eyal Taub
Document by:	MECAL, Enschede, the Netherlands
Number of pages:	88
Keywords:	Mecal B.V., Wind turbine, Floating foundation, Design, FEM, Market study

List of changes			
Version	Date	Page	Short description
V1.0	02/01/2015	All	Original report



Family name:	Mertens
Name:	Ramon
Date of Birth:	24 April 1992
Student ID number:	s1110438
Study program:	Master Mechanical Engineering, Applied Mechanics, Design & Construction
Place and period of Internship:	Enschede, 1 October 2014 – 31 December 2014
Company:	Mecal B.V.
Department:	Wind Turbine Design (WTD)
Manager:	Sabrina Dankelmann
Mentor:	Eyal Taub
Institute:	University of Twente
Place of Institute:	Enschede
Faculty:	Faculty of Engineering Technology
Section:	Applied Mechanics
UT supervisor:	Prof. Dr. Ir. A. de Boer



Abstract

Mecal B.V. is an independent engineering company that is specialized in analyzing, consulting, designing and developing of wind turbines. Mecal has patented a system for the transport and installation of Tension Leg Platforms which can be used as floating foundations for wind turbines.

This report presents the assessment for the global design of a Tension Leg Platform (TLP) which fits the transport and installation system. The TLP was designed for a 6MW offshore wind turbine. The purpose of the project is to validate the feasibility of TLP foundations for offshore wind turbines. The assessment is based on modal analysis, stability analyses, fatigue and ultimate strength analyses, cost estimation and a comparison with a TLP design of another company. Beside all analyses, a market study of TLP foundations was conducted.

The design of the mini-TLP structure was created in Solidworks and improved iteratively. The structure is subjected to a permanent buoyancy load which was calculated in Mathcad. The stability, fatigue and extreme loads are according to load data retrieved from the 6MW wind turbine. Wave loading was taken into account by the use of a safety factor. All analyses were performed with the use of Ansys.

The structure showed small spots with insufficient strength, but can be increased locally with simple solutions. These problems will be addressed when a detailed design is made.

Besides the local insufficient strength and some recommendations regarding further research, the TLP foundation shows good stability, sufficient strength globally, is cost efficient and competitive with other foundations. Therefore, it can be concluded that the design of the mini-TLP foundation is a feasible solution for offshore wind turbines.

Author: R. Mertens

Keywords: Mecal B.V., Wind turbine, Floating foundation, FEM, Market study



Preface

After four years of studying, which was a combination of working hard and being a typical lazy student, the time had come to start an internship to see where the actual work is done. This Internship was the ideal change to bring the learned theory into practice and gain some practical experience in the working field of a mechanical engineer.

After mentioning at the University that I wanted to start an Internship at the end of 2014, several professors recommended Mecal BV. Mecal has its roots at the University and has still good contacts with the University. When I looked on their website I saw several assignments which were well suited for a mechanical engineering internship. Mecal gave me the opportunity to train and apply my mechanical knowledge and FEM skills. I was also given the opportunity to experience a true work environment of a mechanical engineer among an international group.

I started my internship at 1 October 2014 and worked for three months on my assignment. This report will elaborate on the assignment and the things I have done. I would like to thank my professor, internship coordinator and all of my colleges for all their help and support during the internship. Especially, I would like to thank coordinator Sr. Technical Specialist Martin Gemen, Sr. Project Manager Sabrina Dankelmann and my mentor Project Engineer Eyal Taub for their guidance and help during my entire internship.

December, 2014
Ramon Mertens



Content

Abstract	4
Preface	5
Chapter 1 Introduction	9
Chapter 2 The Tension Leg Platform.....	11
Chapter 3 Design references.....	12
3.1 Geometry	12
3.2 Materials	12
3.3 Loads	12
Chapter 4 FE model and calculations.....	13
4.1 General.....	13
4.2 FE model.....	13
4.2.1. Component models.....	13
4.2.2. Coordinate system	14
4.2.3. Geometry	14
4.2.4. Element types.....	14
4.2.5. Materials	16
4.3 Boundary conditions and loads.....	16
4.3.1. Boundary conditions	16
4.3.2. Loads	17
4.4 Results	17
Chapter 5 Modal analysis.....	18
5.1 Method.....	18
5.2 Allowable frequency range	18
5.2.1. Wind turbine frequencies	18
5.2.2. Ocean wave frequencies	18
5.2.3. Allowable frequency range	18
5.3 Results.....	19
Chapter 6 Stability analysis	20
6.1 Stability criteria	20
6.1.1. Tendon tension verification	20
6.1.2. Linear buckling of tubular members	20



6.2	Results	20
6.2.1.	Tendon tension verification	20
6.2.2.	Linear buckling of tubular members	21
Chapter 7	Fatigue strength calculations	22
7.1	Loads and safety factors.....	22
7.2	Method.....	22
7.2.1.	Fatigue strength	22
7.2.2.	Rainflow counting	23
7.2.3.	Palmgren-Miner fatigue analysis	23
7.2.4.	Ultimate fatigue	23
7.3	Results	24
Chapter 8	Ultimate strength calculations.....	25
8.1	Loads and safety factors.....	25
8.2	Method.....	25
8.2.1.	TLP structure	25
8.2.2.	Tendons.....	26
8.3	Results	26
8.3.1.	TLP structure	26
8.3.2.	Tendons.....	27
Chapter 9	Cost estimation of TLP design	28
9.1	TLP structure	28
9.2	Tendons.....	29
9.3	Anchors	29
9.4	Total costs of the TLP	31
Chapter 10	Comparison Design	32
Chapter 11	Conclusion & Recommendations	33
11.1	Conclusion	33
11.2	Recommendations	34
References.....		35
Appendix A	Market Study.....	36
Appendix B	Method and initial design	44
Appendix C	FE Pipe Model APDL	47
Appendix D	FE Shell Model APDL	49



Appendix E	FE model input	50
Appendix F	FE model plots.....	52
Appendix G	FE calculation result plot	55
Appendix H	Ocean wave frequencies	61
Appendix I	Mode shapes	63
Appendix J	Tendon tension results.....	64
Appendix K	Buckling stability results.....	66
Appendix L	Equivalent load ranges	69
Appendix M	Extreme loads.....	70
Appendix N	Fatigue strength results	71
Appendix O	Fatigue strength calculation output.....	73
Appendix P	Ultimate fatigue strength results	75
Appendix Q	Ultimate fatigue strength calculation output	77
Appendix R	Ultimate strength results	79
Appendix S	Ultimate strength calculation output.....	82
Appendix T	Mathcad Calculation	83
Appendix U	Unused models and analyses.....	87

Figure on the front page: Mini-TLP geometry for a 6MW wind turbine



Chapter 1 Introduction

In this report, executed by Ramon Mertens and commissioned by MECAL, a feasibility research of a mini-Tension Leg Platform foundation for an offshore wind turbine is described. This document is made in a project with MECAL reference 10200494 commissioned by MECAL, based on studies performed at MECAL. All information in this document is confidential.

Offshore wind farms hold a great potential as renewable source of energy. However, nowadays an offshore wind turbine has a LCOE (levelized costs of energy) almost twice of that of an onshore wind turbine. The higher costs of offshore wind turbines compared to onshore are mainly from the fixed foundations of the wind turbines which have to be connected to the seabed and require a lot of material and expensive offshore cranes.

An alternative for fixed foundations are floating foundations, which are a relatively new concept and can reduce the material cost drastically. The mini-TLP (Tension Leg Platform) seems to have the biggest potential to reduce the LCOE (levelized costs of energy) of an offshore wind farm. However, a disadvantage is the installation and transportation, which is complex and expensive.

In order to make offshore wind turbines more competitive, Mecal has patented the ITS system which has great potential to lower the LCOE of offshore floating wind turbines. This system is a structure which transports and installs a mini-TLP, saving a lot of transportation and installation costs. The ITS (Installation and Transportation Structure) and the mini-TLP itself must however be checked for feasibility. A global design for a mini-TLP has been made and a stress and stability assessment has been performed.

The calculations are performed on the design of a Tension Leg Platform foundation for a 6MW offshore wind turbine. The 6MW offshore wind turbine is designed as a three-bladed, pitch-controlled upwind wind turbine and will be placed on an offshore floating foundation, the Tension Leg Platform (TLP). The TLP foundation has been designed in global sense, meaning that connections of components are not designed in detail. This assessment can be seen as a validation of the feasibility of a TLP foundation for an offshore wind turbine. The performed calculations will therefore be used as indication, not as full verification.

The TLP calculations are carried out by means of the Finite Element Method (FEM), in order to determine the eigenfrequencies, to check the stability of the structure and to determine the unit stresses for the relevant unit load cases.

A modal analysis has been performed to retrieve the eigenfrequencies of the TLP. The eigenfrequencies are checked for interference with the operating range of the wind turbine and the ocean.

Two stability analyses are performed on the TLP: a tendon tension analysis and a buckling stability analysis. The displacement stability uses the slacking of the tendons as criterion. For the buckling stability a load factor of 1.2 is used as criteria.



Fatigue and ultimate strength calculations are performed for all nodes of the TLP structure by making use of the MECAL program ProDurA® version 2.11.0, which linearly combines the FE unit stresses with the loads released by MECAL WTD, described in ref. [6]

For fatigue, the stress reserve factors (SRFs) are determined using the Palmgren-Miner rule, taking into account a stress concentration factor of 1.00 [-], a consequence of failure factor of 1.15 [-], a material factor of 1.10 [-] and a wave load factor of 1.20 [-].

Peak stresses from the FE calculations are directly applied in the fatigue analysis, applying a stress concentration factor of 1.00 [-] in the fatigue assessment.

For the ultimate strength assessment, the stress reserve factors (SRFs) are determined using the yield strength as criterion, taking into account a material factor of 1.10 [-]. A load factor is included in the loads. An additional wave load factor of 1.20 [-] is used in order to account for the ocean loads.

A cost estimation of material and production of the designed mini-TLP has been performed. A comparison between Mecal's mini-TLP design and that of another company has been made, in order to see if the design will be competitive and feasible. This is done based on the comparison of the found properties.

The contents of this report are as follows. Chapter 2 gives a short introduction to the Tension Leg Platform. In Chapter 3 all the references used to build the FE models and perform the strength calculations are listed. In Chapter 4 the FE calculations are described. Chapter 5 will discuss the performed modal analysis. In Chapter 6 the stability of the TLP is described. Subsequently, Chapter 7 discusses the fatigue strength assessment. In Chapter 8 the ultimate strength calculation is described. Chapter 9 contains a cost estimation of the designed mini-TLP. In Chapter 10 the design will be compared with a TLP design of another company. Chapter 11 will give a conclusion about the performed analyses and assessments and will give recommendations regarding future work. In Appendix A the market study is described, followed by the design method in Appendix B to Appendix D.

Chapter 2 The Tension Leg Platform

The Tension Leg Platform (TLP) is a floating structure, moored by tendons which connect the structure to the sea bottom. The position of the structure is secured by these tendons which are subjected to tension due to the excessive buoyancy of the floating structure. Basically, the structure wants to move upwards, but is kept (partly) under the sea level by the tendons. This results in a very stable platform with greatly reduced upward motion and significant reduced horizontal motion.

The TLP foundation is especially cost efficient for deep water applications, since the construction is relatively small and has a limited height, but the TLP foundation can also be used in moderate sea depths. The stability is achieved by the tendons or tension legs and therefore far less material is needed to anchor the wind turbine to the seabed, compared to other foundations. The TLP foundation has the closest stiffness to a land based system compared with other floating foundations and requires the least effort for strengthening the turbine (ref. [1]). Therefore the TLP foundation is seen as the best cost efficient floating foundation, especially for deeper water applications.

The structures of the TLP can be divided into two groups: a mini-TLP and a 'normal' TLP. The working principle of the TLP and the mini-TLP are the same, however some major differences are present. The mini-TLP is much smaller and lighter than the TLP. This weight reduction is achieved by omitting heavy stabilization columns. The advantage of the mini-TLP is its low weight and therefore a more low-cost solution in terms of material usage. However, the disadvantage is that the mini-TLP is instable for transportation with the turbine attached, whereas the TLP could be transported as a whole. Transportation and installation of the mini-TLP requires an expensive offshore crane. However, this disadvantage is not present with Mecal's ITS.

The stability of a TLP and a mini-TLP is comparable when installed. A TLP and a mini-TLP solution can be seen in Figure 1. The conducted market study on TLP foundations can be found in Appendix A.

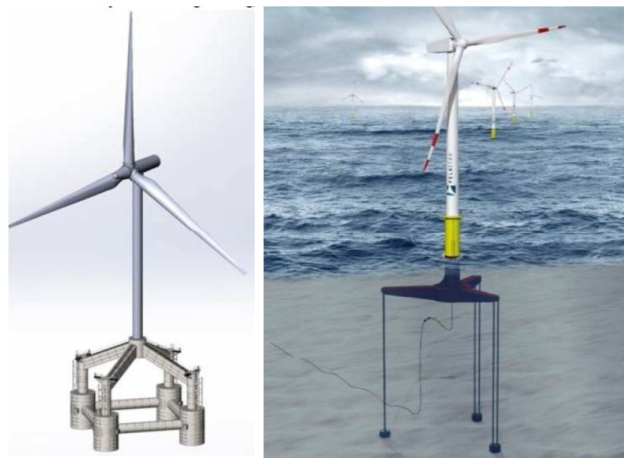


Figure 1: TLP Gicon (Left) and mini-TLP Glosten Associates (right)



Chapter 3 Design references

A basic design of a mini-TLP foundation has been made. For the design several references were used, which will be described in this chapter. The design method used to get to this design can be seen in Appendix B, Appendix C and Appendix D.

3.1 Geometry

- TLP structure: *mini-TLP_structure_v8.x_t*, November 2014 (ref. [1]).
- Tendons: tendon length and angle chosen arbitrarily (see paragraph 4.2.3).

3.2 Materials

- TLP structure: S355J0 according to EN-10025-2 (ref. [3]).
- Tendons: Tendons used according to DNV-OS-E304 offshore standard (ref. [4]).

3.3 Loads

- External loads: 6MW offshore wind turbine data received from MECAL WTD in October 2014 (ref. [6]).
- Buoyancy force: Applied as acceleration. Value calculated according to the displaced volume (Appendix T).
- Wave loads: Wave load factor of 1.20 (ref. [8]).

Chapter 4 FE model and calculations

4.1 General

In this chapter the FE calculations on the TLP structure are described. The FEM computer program ANSYS version 15.0, as distributed by ANSYS Inc. (Houston USA), is used for this purpose. The calculations are done according to non-linear static theory.

4.2 FE model

4.2.1. Component models

The mini-TLP structure (version v02_09, ref. [1]), is built first. The tendons are added as separate components in Ansys. The project is in a predesign stage and therefore only a basic model is built. Joints are not designed in detail. This will be done in a later stage of the project.

The mini-TLP structure with components names and the main dimensions are shown in Figure 2.

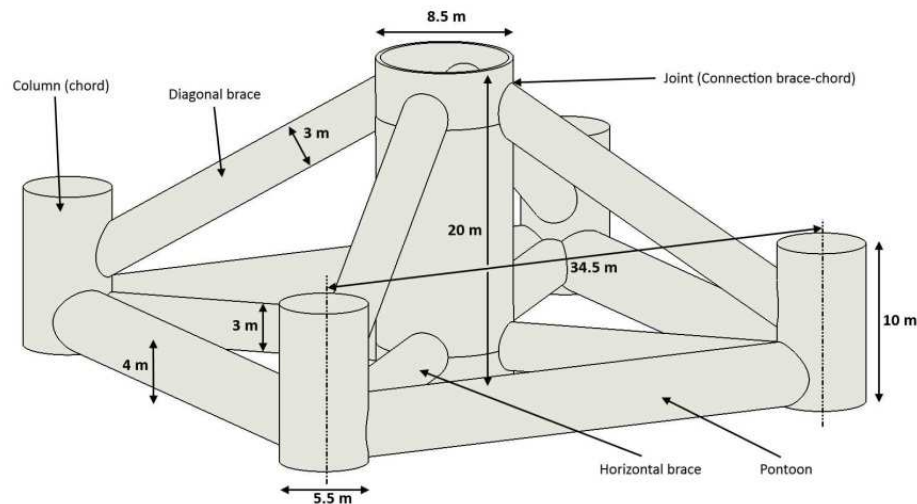


Figure 2: TLP structure with component names and main dimensions

The TLP model is shown in Figure 3.

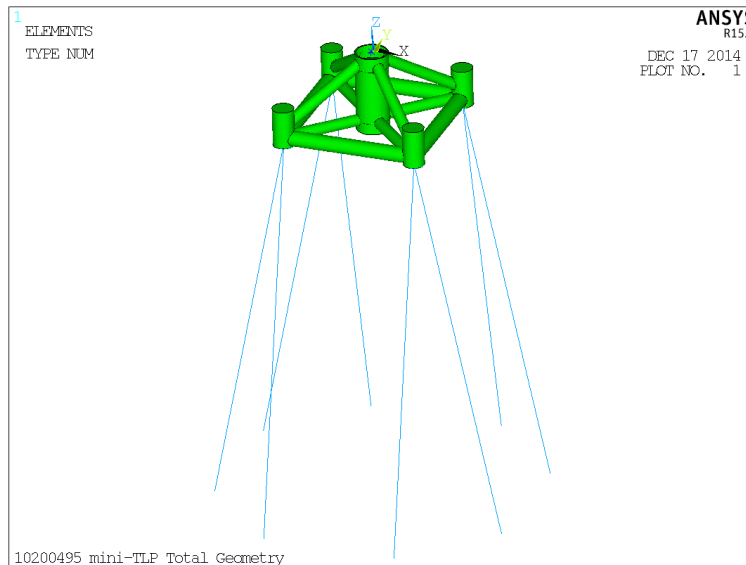


Figure 3: TLP component model

4.2.2. Coordinate system

The global coordinate system is defined:

- Origin at the structure top centre
- X-axis horizontal, pointing in downwind direction
- Y-axis horizontal, pointing left looking from an upwind position
- Z-axis vertical, pointing upwards and perpendicular to the X- and Y-axis

4.2.3. Geometry

The TLP geometry is imported from a CAD model. The simplified tendons are parametrically modelled in ANSYS, according to pre-assigned dimensions. These dimensions are listed in Table 1.

Table 1: Properties of the tendons

Distance seabed – structure	100	[m]
Angle	11.5	[°]
Total length	102	[m]
Cross sectional area	0.0184	[m ²]

4.2.4. Element types

The structure is automatically divided into nodes and elements using the mesh generator in ANSYS. The number of nodes and elements in the model are listed in Table 2.

Table 2: Overview of elements and nodes in TLP Structure FE model

Model	# Elements	# Nodes
V02_09	10,029	27,330

For the TLP structure, structural shell elements are used (SHELL281). These shell elements have quadratic displacement behaviour and are well suited for (relative) thin walled 3D constructions. The elements have six degrees of freedom (translations in nodal x-, y- and z-direction and rotation around nodal x-, y- and z-axis) at each of their nodes (four corner nodes and four mid-side nodes).

The tendons are modelled using 3D spar elements (LINK180). The spar element is a uniaxial tension-compression element and is defined by two nodes with three degrees of freedom at each node (translations in nodal x-, y- and z-direction). The tendons have a line division of one.

The tendons and the structure are connected with the use of BEAM188 elements. These beam elements have two nodes with the same six degrees of freedom as the nodes of the shell elements. The BEAM188 are chosen to be very stiff and with a very low density in order to form a connection which does not deform a lot, but without having a large impact on the total weight of the structure. A mesh plot of the structure and of the beam connection is shown in Figure 4 and Figure 5.

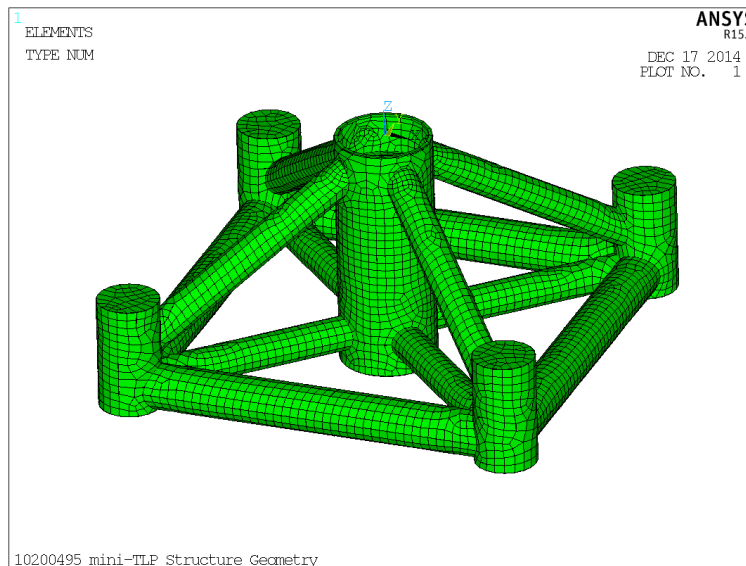


Figure 4: TLP structure component model, mesh plot

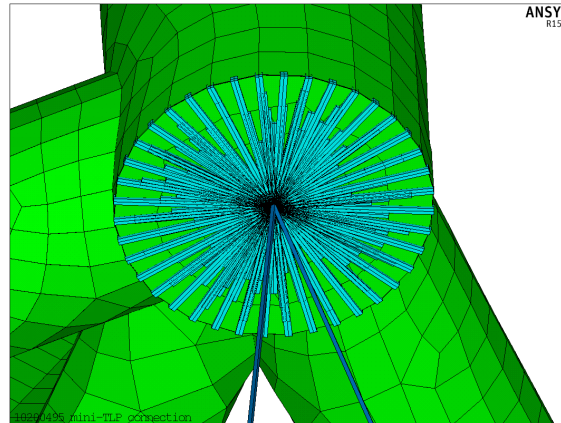


Figure 5: TLP structure and tendon connection through BEAM188

A coarse mesh of the TLP structure will be used in the pre-design stage. A more fine mesh will be used in the detailed design stage of the project.

4.2.5. Materials

The material properties of the TLP structure (as specified in section 3.2) are listed in Table 3.

Table 3: Material properties structural steel S335 [3].

Elasticity (Young's modulus)	E	$2.10 \cdot 10^{11}$	[Pa]
Poisson's ratio	ν	0.30	[-]
Density	ρ	7,850	[kg/m ³]
Yield strength	R_e	$3.35 \cdot 10^8$	[Pa]

Steel wire rope will be used for the tendons. A six strand steel wire rope is selected with a construction group of 6 x 36 and its properties are listed in Table 4.

Table 4: Material properties of one six strand steel wire rope 6x36 group [4]

Elasticity (Young's modulus)	E	$1.95 \cdot 10^{11}$	[Pa]
Mass per length	m	48.8	[kg/m]
Yield strength	R_e	$1.5 \cdot 10^9$	[Pa]

4.3 Boundary conditions and loads

4.3.1. Boundary conditions

The boundary conditions are applied at the bottom nodes of the tendons, which are connected on the seabed of the ocean. For these nodes, zero displacement is specified. The boundary conditions are shown in Appendix F.



4.3.2. Loads

The structure is under a constant buoyancy load, since it has a submerged volume. For all analyses, this buoyancy force must be present. Furthermore, the weight of the tower and the weight of the structure itself have to be taken in account, since they are present all the time. As mentioned in section 3.3, the buoyancy force and the weight are applied as acceleration.

The stability analysis requires the extreme external forces, which can give a good indication for the stability of the structure.

Unit loads are applied on the structure for the Fatigue and Ultimate strength analysis and applied as follows:

- TLP top centre forces F_x , F_y and F_z ($1 \cdot 10^6$ [N])
- TLP top centre moments M_x , M_y and M_z ($1 \cdot 10^6$ [Nm])

Besides the wind turbine loads, waves have also an impact on the structure and should be taken into account. Since these loads could not be calculated accurately, a conservative safety factor will be implemented, as will be discussed in section 7.1 and section 8.1.

4.4 Results

The calculation results include the unit stresses at the nodes of the TLP. Plots of the Von Mises/equivalent stress are shown in Appendix G.

In Table 5 the calculated mass of the TLP structure is listed, as determined in the FE component model.

Table 5: Calculated mass of the TLP structure

Component	Calculated mass [kg]
TLP structure	958,372
TLP including tendons	1,041,071



Chapter 5 Modal analysis

5.1 Method

A modal analysis is done in order to find the natural frequencies of the TLP foundation. This is done with a pre-stressed modal analysis. Pre-stress is achieved by the buoyancy force, which is applied on the foundation and then solved in a static analysis. Subsequently, this (pre-stressed) static analysis is used for the modal analysis. The pre-stressed analysis is needed, because the natural frequencies are depending on the tension in the tendons.

5.2 Allowable frequency range

5.2.1. Wind turbine frequencies

The natural frequencies of the TLP should not overlap the operating frequency range of the turbine. This operating range can be divided in two governing ranges.

First, there is the rotation of the rotor with a rotational speed within a certain frequency range. This range is from cut-in rotational speed to the rated speed. This frequency range is called the 1P range.

Second, there is the passing of a rotor blade in front of the tower. Since most of the wind turbines have a rotor with three blades (which is also the case for the WT), this is called the 3P range.

5.2.2. Ocean wave frequencies

The frequency range of the waves has to be taken into account. These frequencies were determined according to DNV-RP-C205 (ref. [7]). A detailed method is described in Appendix H.

5.2.3. Allowable frequency range

The operation range of the wind turbine and the distributed ocean wave frequencies are combined in one graph in order to see the allowable natural frequency range for the TLP. This graph is shown in Figure 6.

In Figure 6 the operation range of the wind turbine is represented in blue, with the frequency boundaries given in red. The operating range is determined with the minimal and maximal rotational speed of the rotor with a 5% safety margin included. The ocean frequencies are given in orange.

Three ranges for the first natural frequencies are defined: A soft-soft range, a soft-stiff range and a stiff-stiff range. The soft-soft range is not a safe range for natural frequencies since the wave frequencies are present in almost this whole range.

5.3 Results

Natural frequencies of the TLP determined using Ansys, are listed in Table 6. The mode shape plots of these natural frequencies can be found in Appendix H.

Table 6: First natural frequencies of the TLP foundation

Mode nr.	Natural frequency [Hz]
1	0.295*
2	0.559

*a second mode with the same natural frequency was found due to symmetry of the structure.

The natural frequencies of the TLP are in within safe range. The natural frequencies and allowed ranges can be seen in Figure 6.

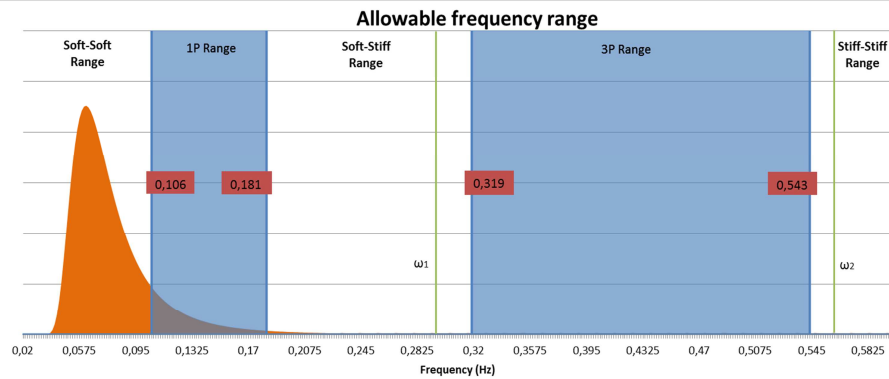


Figure 6: Allowable natural frequency range for the TLP

Chapter 6 Stability analysis

6.1 Stability criteria

6.1.1. Tendon tension verification

The TLP foundation is checked for displacement stability in order to see what the structure can handle in terms of displacement, without collapse. This displacement stability check will be based on the tension of the tendons. All tendons must be tensioned all the time.

Two load cases will be applied:

- Load case 1: a force F_x of the governing extreme load case and increased with factor 10 in 100 sub steps.
- Load case 2: a moment M_y of the governing extreme load case and increased with factor 10 in 100 sub steps.

These two load case are the most governing in terms of stability of the structure. Therefore, forces or moments in other directions are not taken into account for the displacement stability analysis.

6.1.2. Linear buckling of tubular members

Beside the displacement stability, the TLP is checked for buckling stability. This linear buckling analysis will be done by applying the governing forces and moments of all the extreme loads as can be found in Appendix M. The results will be given in a load factor, by which the loads can be multiplied before causing buckling. This load factor must be at least above 1.2 to be in the safe range.

6.2 Results

6.2.1. Tendon tension verification

The factors of the two load cases for which the TLP is still stable in the tendon tension analysis, are given in Table 7. The axial stress of the tendons for load case 2 just before becoming slack is shown in Figure 7.

Table 7: Factor of original load before a tendon becomes slack

Load case	Load	Factor
1	F_x -1,757,110 [N]	1.8
2	M_y -173,993,000 [Nm]	1.5

More plots with the axial stress of the tendons and the total displacement of the TLP can be seen in Appendix J.

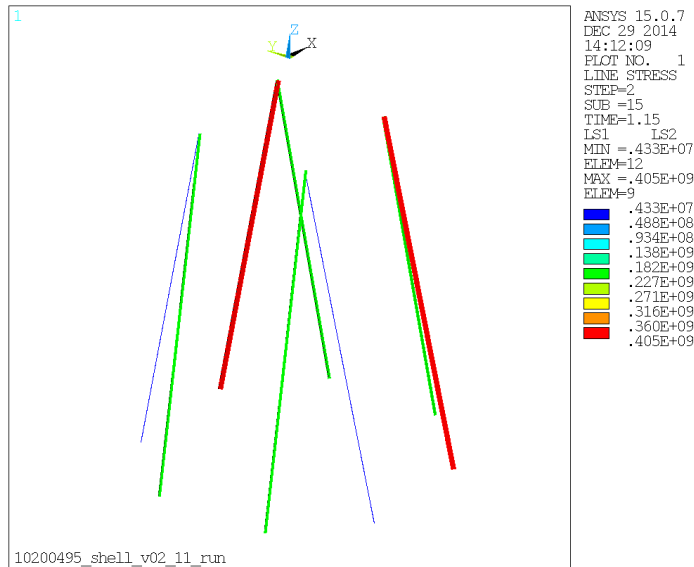


Figure 7: Axial stress for load case 2 within stability criteria

6.2.2. Linear buckling of tubular members

The lowest load factor for which buckling occurs is listed in Table 8. The buckling modes corresponding to these load factors can be found in Appendix K.

Table 8: Overall lowest buckling load factors for the TLP structure

Buckling mode	Load factor
1 st flange	3.31
1 st tubular	10.50

The first buckling mode is found in the lower stiffener ring in the main column of the structure and buckles at a relative low buckling load factor. The buckling of this ring can be easily prevented by adding an additional flange. The first tubular buckling mode is found for a much larger buckling load factor and therefore the structure has sufficient buckling stability.



Chapter 7 Fatigue strength calculations

7.1 Loads and safety factors

There are 993 fatigue load cases for load set v01 (ref. [6]). Forces and moments are applied at the top centre of the structure. The fatigue strength calculations are only performed at the TLP structure itself, the tendons are not taken into account.

The safety factors applied in the analysis are conforming IEC61400-1 standard and are listed in Table 9. Since wave loads could not be calculated or derived, a safety factor which accounts for the wave loads is incorporated. This safety factor is based on the results of offshore design calculations (ref. [8]).

The allowable fatigue damage is 1.00 [-], over the specified lifetime of 20 years.

Table 9: Fatigue strength assessment partial safety factors

Load factor γ_f [-]	Material factor γ_m [-]	Consequence of failure factor: γ_c [-]	Wave load factor γ_w [-]	Total safety factor γ_{tot} [-]
1.00	1.1	1.15	1.2	1.518

7.2 Method

7.2.1. Fatigue strength

In the fatigue strength assessment of the TLP structure a stress conversion is done. For each shell node, three stress components are extracted from the FE model for each unit load case. Next, for each individual stress component and each load case, the unit stress is multiplied with the corresponding load signal at each time step. Finally, for each stress component the resulting stresses of all load components are combined according to the following stress functions:

$$\begin{aligned}\sigma_x(t) &= s_{x_{F_x}} \cdot F_x(t) + s_{x_{F_y}} \cdot F_y(t) + s_{x_{F_z}} \cdot F_z(t) + s_{x_{M_x}} \cdot M_x(t) + s_{x_{M_y}} \cdot M_y(t) + s_{x_{M_z}} \cdot M_z(t) \\ \sigma_y(t) &= s_{y_{F_x}} \cdot F_x(t) + s_{y_{F_y}} \cdot F_y(t) + s_{y_{F_z}} \cdot F_z(t) + s_{y_{M_x}} \cdot M_x(t) + s_{y_{M_y}} \cdot M_y(t) + s_{y_{M_z}} \cdot M_z(t) \\ \tau_{xy}(t) &= s_{xy_{F_x}} \cdot F_x(t) + s_{xy_{F_y}} \cdot F_y(t) + s_{xy_{F_z}} \cdot F_z(t) + s_{xy_{M_x}} \cdot M_x(t) + s_{xy_{M_y}} \cdot M_y(t) + s_{xy_{M_z}} \cdot M_z(t)\end{aligned}$$

With:

$F_x \dots M_z$	Force/moment components in the structure coordinate system [kN], [kNm]
$s_{i_{F_x}} \dots s_{i_{M_z}}$	Normal stresses in i-direction (i = x, y or z) due to each unit load Component [Pa/kN], [Pa/kNm] or [Pa/ms ⁻²]



$s_{j_{Fx}} \dots s_{j_{Mz}}$	Shear stresses in j-plane (j = xy, xz or yz) due to each unit load Component [Pa/kN], [Pa/kNm] or [Pa/ms ⁻²]
t	Time [s]
σ_x, σ_y	Normal stresses in x- and y-direction [Pa]
τ_{xy}	Shear stresses in xy-plane [Pa]

The Von Mises/equivalent stress can be determined with the following equation:

$$\sigma_v(t) = \sqrt{(\sigma_x(t))^2 - \sigma_x(t) \cdot \sigma_y(t) + (\sigma_y(t))^2 + 3 \cdot (\sigma_{xy}(t))^2}$$

7.2.2. Rainflow counting

The stress time signal obtained from all load cases, is rainflow counted to determine the binned number of occurrences for different combinations of stress cycle ranges and mean stress values (the stress spectrum). The rainflow counting is performed by version 2.11.0 of the MECAL program ProDurA®.

7.2.3. Palmgren-Miner fatigue analysis

The stress spectra at the assessed nodes are the input for the Palmgren-Miner fatigue damage calculations by ProDurA®. In this program the S-N curve is applied.

For all locations a conservative wall thickness and associated yield and ultimate strength of respectively 335 [MPa] and 470 [MPa] are used.

Peak stresses from FEM are directly applied in the fatigue analysis, applying a stress concentration factor of 1.00 [-] in the fatigue assessment.

The fatigue strength at each of the assessed nodes is presented by means of stress reserve factor for fatigue (SRF_{fat}), defined as the factor with which the occurring stresses or loads can be multiplied in order to get a total damage of 1.00 [-] in 20 years. For sufficient fatigue strength, the SRF_{fat} value should therefore be equal to or larger than unity.

7.2.4. Ultimate fatigue

The S-N-curves for the TLP structure defined in the previous section do not include the upper fatigue limit or ultimate fatigue strength. Therefore, a separate check is performed to verify if this limit is exceeded by performing an ultimate strength assessment for the fatigue time series.

For this ultimate fatigue assessment, the FE unit stresses are first combined with the fatigue time series as described in paragraph 7.2.1. Next, for the normal stress time series the absolute maximum normal stress $|\sigma_x|_{max}$ for the spots is determined and compared to the yield strength (Re) of the material, taking into account the applicable safety factors:



$$SRF_{ultfat} = \frac{Re}{\gamma_f \cdot \gamma_m \cdot \gamma_w \cdot |\sigma_x|_{max}}$$

With:

γ_f	Load factor [-]
γ_m	Material factor [-]
γ_w	Wave load factor [-]
$ \sigma_x _{max}$	Absolute maximum normal stress [MPa]
Re	Yield strength [MPa]

For all spots a conservative plate thickness of 40-63 [mm] and associated yield and ultimate strength of respectively 335 and 470 [MPa] (ref. [3]) are used in the ultimate fatigue strength calculation.

Spots for which insufficient ultimate fatigue strength is calculated are loaded such that the yield strength of the material is locally exceeded. At these locations a low number of stress cycles may lead to material failure.

7.3 Results

Fatigue strength results calculated with ProDurA®, are listed in Table 10. It has also been checked that the upper fatigue limit is not exceeded.

Table 10: Lowest TLP structure fatigue strength

Location	SRF _{fat} [-]	SRF _{ultfat} [-]
Node 1502	1.185	1.232
Node 6077	0.566	8.594

SRF result plots for the TLP structure fatigue and ultimate fatigue strength can be found in Appendix N and Appendix P, respectively. The TLP structure does not have sufficient strength to bear the fatigue loads defined in ref. [6] in combination with the wave load factor, since the combined fatigue damage is at some places lower than the allowable damage of 1.00 [-]. The structure has sufficient ultimate fatigue strength, since they all values are above unity.

Most of the locations with low fatigue strength occur on local spots and are due to singular points and coarse mesh. Improvement of the fatigue strength on these locations will be done in the detailed design phase of the project.



Chapter 8 Ultimate strength calculations

8.1 Loads and safety factors

In the ultimate/extreme strength calculation, the ultimate load set from ref. [6] is used. The forces, moments in the load cases from the ultimate load set are applied at the structure top centre. The ultimate strength calculations are performed on the TLP structure, a separate ultimate strength analysis is done for the tendons.

The partial safety factors that are applied in the analysis are listed in Table 11. Since wave loads could not be calculated or derived, a safety factor which accounts for the wave loads is incorporated. This safety factor is based on the results of offshore design calculations (ref. [8]).

Table 11: Ultimate strength assessment partial safety factors

Load factor * γ_f [-]	Material factor γ_m [-]	Wave load factor γ_w	Total safety factor γ_{tot} [-]
1.00	1.10	1.2	1.32

*The load factor is already included in the loads ($\gamma_f = 1.35$)

8.2 Method

8.2.1. TLP structure

The calculation of the ultimate strength SRFs (SRF_{ext}) is similar to the description in section 7.2.4. First, component stresses are calculated from the FE model unit stresses. These are then combined with the load component values from the extreme load cases. Instead of rainflow counting as performed in the fatigue analysis, the maximum occurring Von Mises stresses are used in the ultimate strength calculation.

The ultimate strength SRF, which is defined as the ratio between the occurring stresses and the allowable stresses, is then calculated as follows:

$$SRF_{ext} = \frac{Re}{\gamma_f \cdot \gamma_m \cdot \gamma_w \cdot |S|_{max}}$$

With:

γ_f	Load factor [-]
γ_m	Material factor [-]
γ_w	Wave load factor [-]



$ S _{\max}$	Absolute maximum Von Mises stress [MPa]
Re	Yield strength [MPa]

8.2.2. Tendons

The calculation of the ultimate strength SRFs (SRF_{ext}) of the tendons is different from that for the TLP structure. Governing load sets as found in Appendix M are applied. The axial stress in the tendons is investigated for these governing load sets, with use of FEM.

The ultimate strength SRF, which is defined as the ratio between the occurring stresses and the allowable stresses, is then calculated as follows:

$$SRF_{ext} = \frac{Re}{\gamma_f \cdot \gamma_m \cdot \gamma_w \cdot |S|_{\max}}$$

With:

γ_f	Load factor [-]
γ_m	Material factor [-]
γ_w	Wave load factor [-]
S_{\max}	Maximum axial stress [MPa]
Re	Yield strength [MPa]

8.3 Results

8.3.1. TLP structure

The ultimate strength results for the TLP structure, calculated using MECAL software ProDurA® version 2.11.0, are listed in the Table 12.

Table 12: Overall lowest ultimate strength TLP structure

Location	SRF_{ext} [-]
Node 1502	0.801
Node 793	0.830
Node 1390	0.899
Node 1593	0.948
Node 4579	0.949

SRF result plots for the TLP structure ultimate strength can be found in Appendix R. It is concluded that the TLP structure does not have sufficient strength to bear the ultimate loads according to ref. [6] with all safety factors included. The troublesome areas, as the connections of the braces will have to be locally thickened or a better stress distribution has to be realised.



8.3.2. Tendons

The ultimate strength result for the tendons for the governing load case (ua62_42.5_709ea) is listed in Table 13.

Table 13: Overall lowest ultimate strength tendons

Location	SRF _{ext} [-]
Tendon 1	3.392

SRF result plots for the tendons ultimate strength can be found in Appendix R. It is concluded that the tendons have sufficient strength to bear the ultimate loads with all safety factors included.



Chapter 9 Cost estimation of TLP design

A global design has been made for a mini-TLP for a 6MW offshore wind turbine. A strength and stability assessment has been performed on the geometry as can be found in the previous chapters. The results showed that the global design was already feasible, with only some minor improvements needed in order to give it sufficient strength. It is interesting to compare the properties of the designed mini-TLP with that of another design. But before this will be done, a rough costs estimate will be done on the TLP design.

9.1 TLP structure

The material cost will have a significant share in the total cost of the TLP structure. For the TLP structure, steel will be used. Typical prices for this kind of steel are around 1000 €/ton.

Beside the material costs, the assembly costs will have a major share in the total costs. The structure consists of several large diameter pipes which will be welded together. This is the most expensive process in the production of the TLP structure. The cost for the welding is quite hard to calculate. Therefore costs of other offshore foundations are evaluated:

- For a Jacket structure, which consists of a lot of small diameter pipes, typical costs for welding are around 2500 €/ton of total weight.
- For a monopile structure, which consists of very large diameter pipes, typical costs for welding are around 500 €/ton of total weight.

The cost of welding of the TLP structure will be somewhere between these two cases. The cost for welding the TLP will be taken the same as the costs of welding for jackets and are therefore quite conservative. This is done to account for other costs which may be present in the production of the TLP.

Costs per ton of structure:

Material costs = 1,000 €/ton

Welding costs = 2,500 €/ton

Weight of the structure:

Total weight = 1,000 ton

The total costs for material and production of the TLP structure will be:

Total costs = $3,500 \cdot 1,000 = 3,500,000$ €

9.2 Tendons

Since the tendons will be bought and not a lot of processing is required, the costs of the tendons are based on the specifications of suppliers.

Based on costs of other tendons (experience in ATS b.v.), the cost of a tendon is calculated to be 28400 €/m² per one meter length.

Cross-sectional area of one tendon:

$$A_{\text{tendon}} = 0.0184 \text{ m}^2$$

Cost of a tendon per one meter length:

$$\text{Cost tendon} = 0.0184 \cdot 28400 \approx 522.50 \text{ €/m}$$

Length of one tendon:

$$L_{\text{tendon}} = 102 \text{ m}$$

Total costs of the tendons:

$$\text{Total costs tendons} = 522.50 \cdot 102 \cdot 8 \approx 426,500 \text{ €}$$

9.3 Anchors

Cost estimation will also be done for the anchors, which will be used to connect the tendons to the seabed. Although no definitive choice or design has been made for the anchoring, this will probably be done by the use of a Gravity-based structure (GBS). A GBS is a structure which will be placed on the seabed to which the tendons will be connected. The gravity force of the structure must be more than the upward pulling of the tendons. The GBS can be a quite simple structure made out of reinforced concrete.

The mass of the GBS will be based on the tension force found in the analyses done for the strength and stability assessment. There are several easy ways to design or construct a GBS for the TLP with excessive mass, but with a more optimized design this excessive mass can be reduced. Beside the optimized mass, the positioning of the GBS on the seabed has to be taken in account. This positioning has to be done relative accurate with a tolerance of one meter.

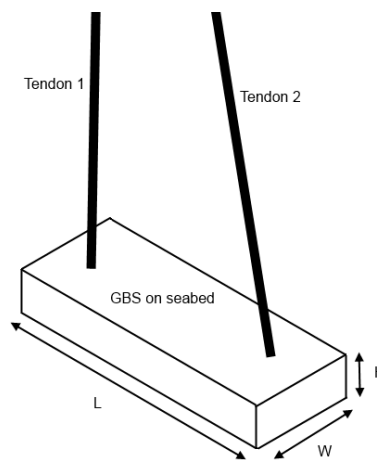


Figure 8: Possible solution for the GBS for the TLP



A possible design can be seen in Figure 8, which will reduce the total required mass of the gravity-based structures and as well reduce the effort needed for the positioning. For each of the four corners of the TLP structure, there will be place such a GBS.

A rough estimation of the required mass of one GBS can be easily calculated when the governing upward forces for extreme conditions of one set of two tendons will be used. This gives:

Governing forces found for the extreme load case:

$$F_{\text{tendon1}} = 4,887,200 \text{ N}$$

$$F_{\text{tendon2}} = 6,237,000 \text{ N}$$

Minimum downward force required to keep the GBS on the seabed.

$$F_{\text{g required}} = F_{\text{tendon1}} + F_{\text{tendon2}} = 11,124,200 \text{ N}$$

The required mass for one GBS:

$$M_{\text{gbs}} = \frac{F_{\text{g required}}}{g} = \frac{11,124,200}{9.81} \approx 1,134,000 \text{ kg} = 1,134 \text{ tons}$$

Total required mass needed for all GBS:

$$M_{\text{total}} = M_{\text{gbs}} \cdot 4 = 4,536 \text{ tons}$$

A quick calculation on the dimensions of one GBS is done to get an idea for the size:

Density of reinforced concrete:

$$\rho_{\text{concrete}} = 2,400 \text{ kg/m}^3$$

Volume of one GBS:

$$V_{\text{gbs}} = \frac{1,134,000}{2,400} = 472.5 \text{ m}^3$$

Possible dimensions for the structure are: 40m x 5m x 2.4m (L x W x H)

The price for reinforced concrete with complex geometry is around 350 €/ton. For simple reinforced concrete structures prices of 150 €/ton can be found. Although the GBS is not a complex structure, the connection of the tendons is not yet taken in account. Therefore the costs are taken quite conservative by taking this high price for reinforced concrete.

Total cost of all GBS:

$$\text{Total costs GBS} = 4,536 \cdot 350 = \text{€ } 1,587,600$$



9.4 Total costs of the TLP

Since all major costs are known, the total costs of the production of the TLP can be determined.

The total costs are determined by adding all costs which are calculated:

$$\text{Total costs} = 3,500,000 + 426,500 + 1,587,600 = 5,514,100 \text{ €}$$

The costs of a foundation are usually expressed in million euros per installed MW:

$$\frac{5,514,100}{6} \approx 0.92 \text{ million €}/\text{MW}$$

The costs calculated are only the costs of the TLP foundation itself. These costs are rough estimates as mentioned before, but will give an insight of what could be expected. Although not every aspect of the production is taken in account, the total costs are expected not to increase a lot since prices for materials and processing are taken conservative.

The costs per installed MW for this design seem high, especially in comparison with fixed solutions for shallow water applications. These prices are around 0.5 million €/MW, however for sites at 25 meter depth (ref. [9]). Increasing the height will increase the costs. Especially for the deeper water applications the mini-TLP will be far better cost efficient.

Installation costs cannot be estimated and are also not of interest, since further research will be performed on the Installation and Transport System of Mecal, which will reduce these costs.



Chapter 10 Comparison Design

As can be seen in the results of previous chapters, the mini-TLP design seems to be a feasible design. Also the costs of the production of the mini-TLP are promising. To give an idea if the design is competitive or realistic, it will be compared with other mini-TLP solutions. Although most companies listed in Appendix A do not give details about the properties of their TLP design, the company Iberdrola did present some details about their Flottek project (ref. [10]). The details found on the Flottek project will be compared with the values for Mecal's mini-TLP design.

The Flottek project was designed for a 5 MW wind turbine, which is expected to have less mass than the 6MW wind turbine.

The properties are compared with each other and are listed in Table 14.

Table 14: Comparison between mini-TLP of MECAL and mini-TLP of Iberdrola

Properties:		Mecal mini-TLP, 6 MW WT	Iberdrola mini-TLP, 5 MW WT
Sea depth	[m]	120	80
Draught	[m]	21	40
Width	[m]	40	64
Steel weight	[kg]	1,005,900*	1,050,000
Displaced mass	[kg]	4,831,000	4,300,000
Cost	[€/MW]	$0.92 \cdot 10^6$	$1.0 \cdot 10^6 - 1.2 \cdot 10^6$ **

*Since the design needs some additional strength locally, the total weight was corrected with factor of 1.05

** From the data given in the reference it cannot be seen if these costs are including the installation or installation system costs

It can be seen that the properties of Mecal's mini-TLP are very promising. Most of the properties are better than the properties found for Iberdrola mini-TLP.

However, these results are not conclusive, since Mecal's mini-TLP is only designed in global. Connections of tendons, weld strength analysis and full dynamic wave behavior are for example not yet analyzed. These analyses are required when the mini-TLP will be designed in detail and may influence the current properties quite drastically. Iberdrola designed and tested their mini-TLP for waves of over 30 meter and thus really proved the capabilities of their mini-TLP design.

Nevertheless, the comparison gives an insight on the competitiveness of Mecal's mini-TLP design.



Chapter 11 Conclusion & Recommendations

11.1 Conclusion

The TLP foundation, designed for a 6MW offshore wind turbine, has been assessed in order to validate the feasibility of the TLP foundation for an offshore wind turbine. The calculations were carried out by means of the Finite Element Method (FEM). This was done in order to determine the natural frequencies, to check the stability of the structure and to determine the unit stresses for the relevant unit load cases.

The following conclusions are made:

- The modal analysis showed that the natural frequencies of the construction do not interfere with the operating frequency ranges of the wind turbine and with the frequencies of the ocean waves. The construction has optimal natural frequencies and does not require any changes.
- For the displacement stability, the tension in the tendons was lost for load case 2 for a load factor of 1.8. Therefore, the structure has sufficient stability for the tendon tension verification.
For the linear buckling stability, the smallest load factor for which tubular buckling occurs was determined to be 10.50. A buckling mode was found in a stiffener ring for a load factor of 3.31, but this structural detail can be easily improved if needed. Furthermore, since the criterion was set to be at a minimum load factor of 1.2; the TLP structure has sufficient buckling stability.
- The fatigue strength calculation, which has been performed, showed some minor problems in the structure. For this calculation the lowest SRF_{fat} value was found to be 0.566, which is not sufficient. However, when the SRF_{fat} values are evaluated for the whole construction, only very small spots where the SRF_{fat} value is below unity can be found. The fatigue strength of these local details can be improved quite easily (ring stiffeners, increased thickness etc.).
In terms of ultimate fatigue strength, the calculations showed sufficient strength. The lowest SRF_{ultfat} was found to be 1.232, which is above unity.
- The ultimate strength calculation showed similar problems as the fatigue strength calculation. The lowest SRF_{ult} calculated value was 0.801 and therefore requires a local improvement of the design. Similar to the fatigue strength, most of the structure has sufficient strength and only local details have insufficient strength. The tendons have sufficient strength.
- The cost estimate of the designed mini-TLP foundation shows quite some costs, however costs estimations were conservative. These costs are not conclusive since transport, installation are not taken in account.



- The comparison between the designed mini-TLP and Iberdrola Flottek project showed promising results for the designed mini-TLP. Most properties were better than that of the Flottek project; however the conclusion will be reticent.

Despite the fact that the design of the TLP did not have sufficient strength, it can be concluded that TLP foundation is a feasible solution for an offshore wind turbine foundation. This insufficient strength was only present in spots near connections and the construction was designed in a global sense, this can be easily addressed and improved in the detailed design phase. The calculations have proved that the structure has sufficient stability and there is no overlap of the natural frequencies and the excitation frequencies.

11.2 Recommendations

Despite being a feasible design, the TLP structure still needs some improvement. Therefore, some recommendations are made in order to address the problems which are still present in the design or other evaluations which need some additional attention:

- A detailed design and analysis of the joints (brace-chord connection), with a refined mesh and local improvement by e.g. locally thickening, adding flanges, adding stiffener rings.
- More detailed calculations of the welds, in combination with the detailed design.
- Check for punching shear of the large pipes with relative thin walls.
- New calculation in order to retrieve accurate loads for the TLP foundation. The load data coming from the 6MW wind turbine (ref. [6]) has been calculated with different foundation stiffness.
- Check the influence of the waves calculated in an accurate way in order to verify if the structure has enough strength to be able to withstand the ocean loads.
- Modelling the stiffness of the ground connections more accurately and checking the influence on the dynamic behaviour of the structure.
- An analysis of the installation of the TLP.
- A collision analysis.
- A damage stability analysis, to see if the structure still holds when the hull is damaged (due to ship collision).



References

- [1] Wybren de Vries, "Final report WP 4.2 - Support Structure Concepts for Deep Water Sites". UpWind, 2011
- [2] TLP Structure CAD model, *mini-TLP_structure_v8.x_t*, MECAL WTD, November 2014.
- [3] DIN EN 10025-2, "Hot rolled products of structural steels Part 2: Technical delivery conditions for non-alloy structural steels", April 2005
- [4] DNV-OS-E304, offshore mooring steel wire ropes, April 2009
- [5] Mathcad buoyancy force calculation, *Mathcad-10200494_mini-TLP_Dimension_Calculation_file_v02.pdf*, Mecal WTD, October 2014
- [6] R. Van Hoof, "*Load report for the 6MW wind turbine GL2005-WTC-IIb*", 10100003-XXXX-589-loadreport_V02_loadset_V1.0.pdf, MECAL WTD, October 2012
- [7] DNV-RP-C205, Environmental conditions and environmental loads, April 2014.
- [8] J. Van Der Tempel, e.a., *Robustness of offshore wind turbine design calculation*, Interfaculty Offshore Engineering & Section Wind Energy Delft University of Technology, -
- [9] We@sea 5.1, "Optimal integrated combination of foundation concept and installation method". presentation We@sea December 2010
- [10] Iberdrola Ingenieria TLPWIND, "*A smart way to drive costs down*". EWEA presentation, 2014
- [11] Wybren de Vries, "Final report WP 4.2 - Support Structure Concepts for Deep Water Sites". UpWind, 2011
- [12] Athanasia Arapogianni and Anne-Benedicte Genachte, "*Deep Water – The next step for offshore wind energy*". EWEA, July 2013
- [13] "Floating Offshore wind Foundations: Industry Consortia and Projects in the United States, Europe and Japan". Main(e) International Consulting LLC, May 2013
- [14] <http://www.blueengineering.com/>
- [15] Javier Pascual, "*EOLIA Project and its outcomes in Deep Offshore Floating Wind Technology*". Technology Development, Wind and Marine Renewable, Maart 2011
- [16] <http://www.seaplace.es/proyecto-eolia/>
- [17] <http://www.windpowermonthly.com/article/1316579/gallery-iberdrolas-floating-platform-design>
- [18] F. Adam, "Experimental Studies and numerical modelling of structural behaviour of a scaled modular TLP structure for offshore wind turbines". GICON, 2014
- [19] Koji Suzuki, Hiroshi Yamaguchi, e.a., "*Initial design of TLP for offshore wind far*". Tokyo Japan, may 2010
- [20] "Ocean Breeze is a Deeper Water Wind turbine Foundation System for The Largest Wind Turbine Towers Sited in Waters up to 200m", Ocean Recourses Ltd, 2012
- [21] <http://www.eti.co.uk/project/floating-platform-system-demonstrator/>
- [22] "*PelaStar Installation and Maintenance, v.01p*". Glosthen Solutions, Inc., Seattle, Washington, February 2012



Appendix A Market Study

A market study has been conducted on the mini-TLPs and the TLPs. This section will show some existing ideas, concepts, designs or prototypes on mini-TLPs and TLPs. Currently none of these floating foundations has been applied on wind farms. However, several companies are developing TLP/mini-TLP structures which will probably be deployed in the nearby future. An overview will be given of the known projects according to ref. [12][13]. Most of the projects are briefly explained and without details, since given information was limited.

Blue H TLP

Company:	Blue H
Foundation:	Mini-TLP
Development:	Development of TLP for a 5 MW turbine Demonstrator model 5 MW was planned 2015, commercial model 2016

General information

Blue H can be considered as the pioneer in the floating foundations for wind turbines. In 2008 they engineered, manufactured, assembled and demonstrated a small prototype, a TLP with an 80kW turbine. This is considered to be the world's first floating foundation. Now Blue H has developed a floating foundation for 5 to 7 MW turbines, for water depths of over 50 meters and harsh marine environment. This TLP consists of one large buoyant hull on which the turbine tower is placed. Attached to this hull are three legs, which are connected to the tendons, which are connected to the foundation (ref. [14]). Unfortunately, it seems that Blue H does not exist anymore.

Transportation and installation

The floating foundation has the wind turbine already installed onshore. The transportation of the structure is done using tugboats only. Detachable stabilizers are used for the transportation and installation. These stabilizers are cylindrical buoyant containers, which are connected to the legs of floating foundation. The stabilizers will be submerged when installing the structure, which will lower the structure to the depth on which the tendons can be connected. With the tendons connected, the ballast will be pumped out of the stabilizers, thus tensioning the tendons, and will then be removed. Transportation and installation can be done in a large weather window, during 2m and 3m mean wave height.

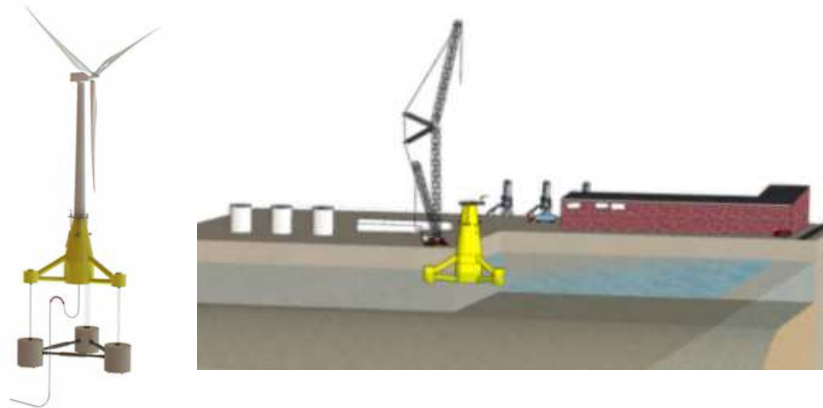


Figure 9: TLP foundation of the Blue H group, with assemblage of the TLP on the right (ref. [14])

Eolia

Company:	Acciona Energy
Foundation:	TLP
Development:	Development and testing of multiple floating foundations, including a TLP foundation

General information

Acciona is developing a spar, a semi-submergible and a TLP platform for deep waters (over 40 meters) all under the project name EOLIA. These floating platforms are already tested for several situations with scale models for water depths of 200 meter. The platforms are designed for a 5 MW wind turbine. The TLP foundation consists of one large buoyant column with three legs attached to it. These legs are connected to the tendons.

Acciona has concluded that there is no optimal solution for floating foundations; however they are now further developing a semi-submergible foundation.

Transportation and installation

Since Acciona has stopped the development of the TLP foundation, information about how transportation and installation would have been done is scarce. Concluding from the scale model tests, it was probably with use of tug boats (ref. [16])

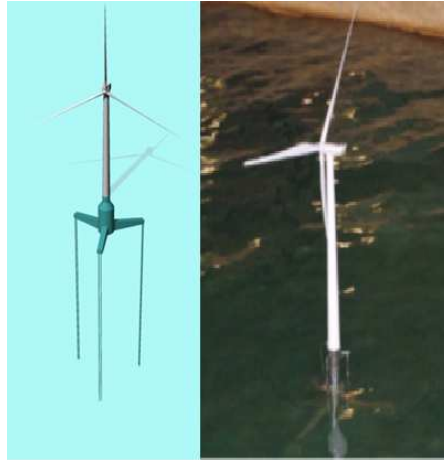


Figure 10: TLP foundation of Acciona's Eolia project (ref. [16])

FLOTTEK

Company:	Iberdrola
Foundation:	Mini-TLP
Development:	Development of two foundations for a 2 MW and 5MW turbine

General information

Iberdrola is developing two TLP variants to be used with a 2MW and 5MW turbine. Turbine OEM partners are Acciona and Alstom. Iberdrola has already tested scale models of these foundations. They also have designed two innovative installation systems for these offshore structures. The floating foundation consists of a buoyant hull on which the tower is placed. Attached to this buoyant hull are four legs or pontoons, which are connected to the tendons. The placing of the turbine tower is done onshore.

Transportation and installation

The transportation of the floating structure will be done using tugboats. During transport extra floats are connected to the pontoons, increasing the buoyancy of the foundation and thus stabilizing the whole structure. When in position the tendons will be connected to the floating foundation. The stabilizing floats will be removed after installation. This process can be seen in Figure 11.

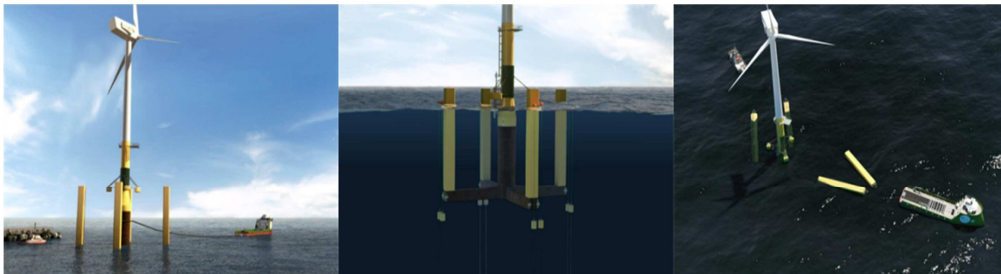


Figure 11: Transportation and installation of FLOTTEK's TLP foundation (ref. [17])

GICON-TLP

Company:	GICON group
Foundation:	TLP
Development:	Development of a prototype for a 2 MW turbine (2014/2015) and a prototype for a 6 MW turbine (2015/2016) Serial production for a 6 MW turbine (2017/2018)

General information

Since 2009 Gicon is developing a TLP platform. Several scale models have been made to prove the capabilities of the TLP. In 2013/2014 they modified their design to an economical solution. Their TLP is deployable from 20 meters to 300 meters. The design consist of four large cylindrical buoyant bodies which are connected to each other with horizontal pipes and cantilever beams which come together at the transition piece. Their 2 MW TLP design is scaled for the 6 MW design (ref. [18]).

Transportation and installation

The GICON TLP together with the wind turbine will be assembled portside and the entire structure will be transported to the deployment location with use of tugboats. Their installation of the tendons will depend on the geology of the location.

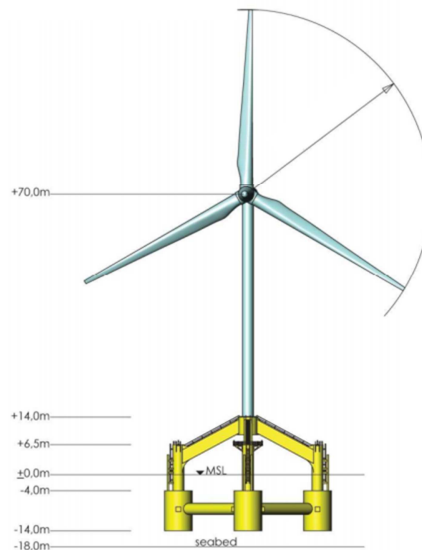


Figure 12: GICON TLP foundation for a 6 MW wind turbine (ref. [18])

Mitsui Zosen

Company:	Mitsui Engineering & Shipbuilding
Foundation:	TLP
Development:	Development of TLP structure Prototype is planned at some stage (year unknown)

General information

Since 2009 Mitsui Engineering & Shipbuilding has been researching and developing a TLP structure. An initial design has been made for a TLP structure for a 2.4 MW wind turbine for an installation site of the Japanese coast. Their TLP structure consists of a center column with three pontoons attached. At the end of each pontoon, a corner column is present to add more buoyancy. The tendons are also connected to these corner columns. Their research also proved the dynamic stability of the TLP design for various wave types (ref. [19]).

Transportation and installation

How the transportation and installation of a TLP will take place, is not known. It is assumed that they will tow the structure to the location, since their structure is very wide.

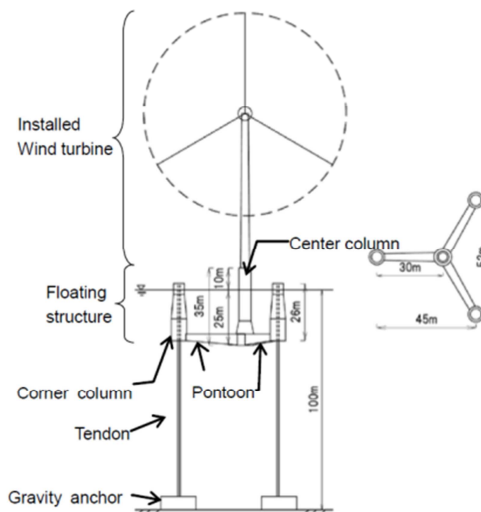


Figure 13: Initial design of Mitsui Zosen TLP foundation (ref. [19])

Ocean Breeze

Company:	Xanthus Energy
Foundation:	TLP
Development:	Commercializing the product Building wind farms 2015/2016

General information

Ocean Breeze is a deeper water wind turbine foundation for large wind turbine towers sited in waters between 60 meters and 200 meters deep. Ocean Breeze uses a buoyant hull and wind turbine support structure consisting of four large watertight buoyancy chambers at each corner, interconnected by a lattice framework with a central wind turbine support column (ref. [20]).

Transportation and installation

Transportation is done by using tugboats, which first transport the floating gravity base to the location and install the base by submerging it. After the base is properly positioned the buoyant structure, with the turbine already in place, is towed to the location, also by tug boats. Once in position, the structure is drawn below the surface by winching cable connected to a pad eye on the foundation. Tendons are then connected and allowed to take the loads from the structure. The operation is expected to take two times eight hour weather windows (ref. [20]).

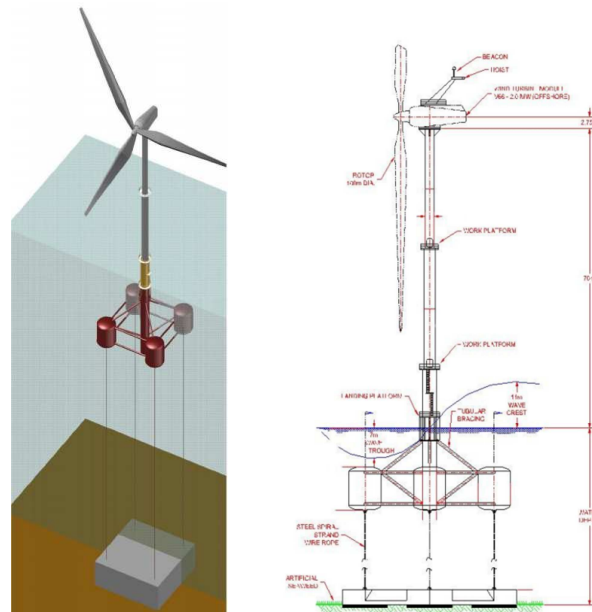


Figure 14: OceanBreeze TLP solution (ref. [20])

PelaStar

Company:	Glosten Associates, Alstom
Foundation:	Mini-TLP
Development:	Commercializing the product 6 MW turbine demonstration model planned for 2015, with multi-unit pilot project following in 2017.

General information

The PelaStar system is a project from Glosten Associates, who are collaborating with Alstom. Alstom has developed the Haliade 150-6, a 6 MW turbine, which will be placed on the PelaStar TLP. The PelaStar TLP system consists of a large buoyant column in the middle with three buoyant legs attached to it. Two tendons are connected at each leg. The wind turbine will be assembled with the PelaStar system in-harbor (ref. [21][22]).

Transportation and installation

The PelaStar is not stable enough for transit by tugboats. The additional buoyancy required for the transportation is achieved by using the PelaStar Support barge. The barge with the TLP will then be towed to location. This barge will also hold all necessary equipment to install the TLP at location (ref. [21][22]).



Figure 15: PelaStar TLP foundation with the Alstom Haliade Turbine (ref. [21])

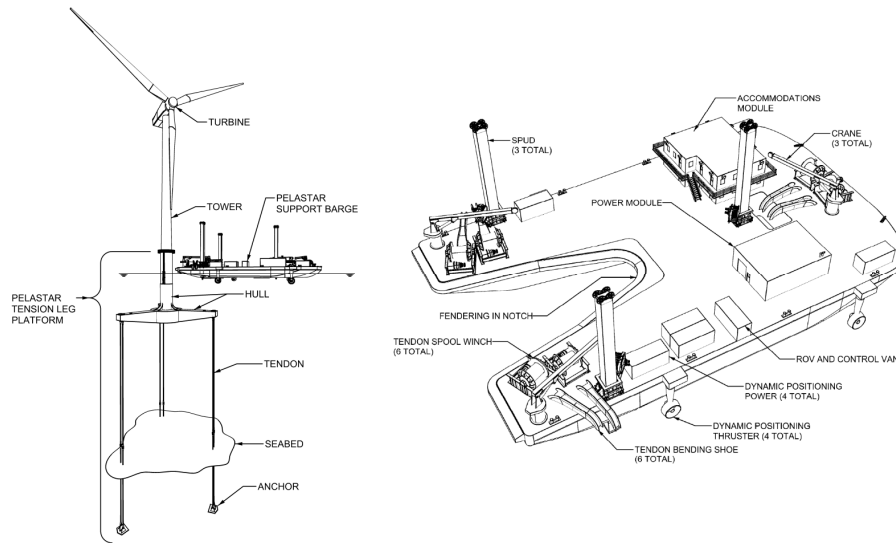


Figure 16: Transportation and Installation of the PelaStar TLP (ref. [22]).

Conclusion market study

Several companies are developing a TLP floating foundation, with phases ranging from idea phase to the prototype phase. Every company has a slightly different view and therefore their approach of how their design is build up. The stages of development vary a lot, but most of the companies are in the testing/prototype phase with plans to build a full scale demonstrator in one or two years. There are companies developing TLP solutions which will be towed to location, but also some companies which are developing mini-TLPs with an additional transportation/installation solution. Especially these latter projects are of interest.

The Flottek project of Iberdrola and the Blue H TLP project of Blue H group both use stabilizing columns for the installation and transportation. This will give the additional stability needed for the transportation; however these stabilizing columns have a very large size. Since these columns must be buoyant for the stabilization, they can become hard to control when uncoupling. Even with use of ballast water, this can be a hazardous operation, since the columns have building sized dimensions.

The PelaStar project uses a barge for the transport and installation. This is a far more reasonable solution then only a few buoyant columns. However this barge has as disadvantage the large costs for the development, production and use of such a barge which has only one purpose. This barge has potential, but also has a large risk.

Mecal's idea will be in between these two solutions. The structure does not have the questionable loose stabilizing columns but also not the expensive and risky investment for a barge.

Appendix B Method and initial design

Iterative approach

A mini-TLP solution has been designed which fits the MECAL idea on a transport and installation solution. An iterative method was used. The design of the mini-TLP was started by performing some analytical calculations, to determine the initial dimensions of the mini-TLP. The performed calculations were made with use of the program Mathcad 14 (ref. [5] or Appendix T). The calculations required actual loads of a wind turbine, (ref. [6]). The dimension achieved with the calculations, were used to build a simple FE model in ANSYS. This FE model was used in analyses which gave strength and displacements results. These results gave feedback to update the geometry until satisfying or sufficient results were achieved. This can be seen in the scheme of Figure 17.

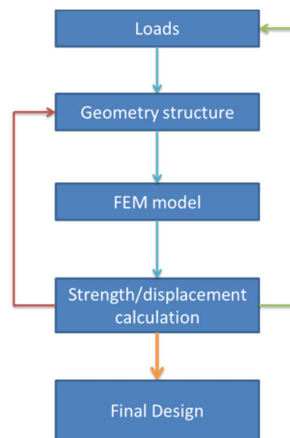


Figure 17: Iterative method used to get the final mini-TLP design

In the scheme a feedback loop is included back to the loads. The stiffness of the structure influences the loads of the wind turbine. These must be calculated again in order to get accurate loads of the wind turbine. Since this is a very time consuming task, this has not been done.

Calculations

The first calculations were based on the geometry shown in Figure 18. This design consists of a large buoyant column and four smaller buoyant columns. These smaller columns are connected with beams and braces.

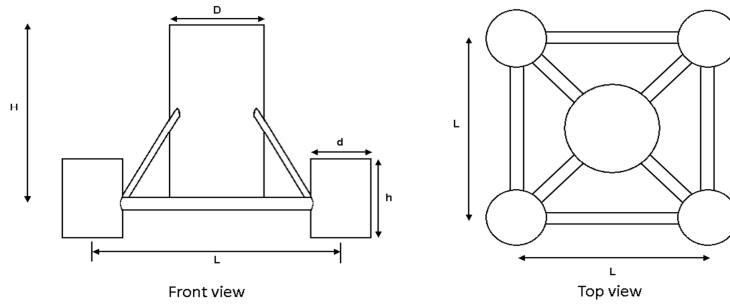


Figure 18: Initial geometry of the mini-TLP

The geometry had to be designed in basic dimensions at first, therefore a 2D Free-Body-Diagram was used to calculate a certain minimum required buoyancy force. This buoyancy force gave a required displaced volume of the structure, which will be converted to the basic dimensions of the structure. The FBD is shown in Figure 19.

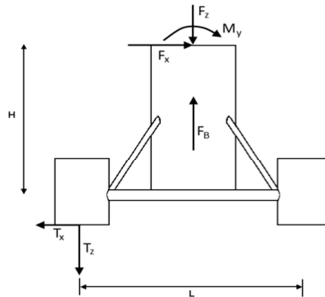


Figure 19: 2-D Free body diagram of the mini-TLP

Equilibrium equations were set up and a minimum required buoyancy force was calculated. These calculations can be seen in ref. [5] or Appendix T.

The buoyancy force by a submerged body is given by displaced mass times the gravitational force, as can be seen in the following formula:

$$F_{\text{buoyancy}} = V_{\text{structure}} \cdot \rho_{\text{seawater}} \cdot g$$

Since the structure consists of simple sized components, the volume of each component was determined and summed (ref. [5] or Appendix T). This gave a minimum required volume. This minimum volume in combination with the initial sketch for the geometry and estimating required and appropriate dimensions to achieve this volume gave the first dimensions.

After a few design iterations it became clear that more buoyancy was needed. This could have been done by increasing the size of the big column and smaller columns, but this would lead to extremely big sized columns which are sensitive to buckling. Therefore, the braces and beams were increased in size, such that they became pontoons and significantly contributed to the total buoyancy of the structure. A sketch of the new geometry can be seen in Figure 20 and was based on the geometry of the CAD model. The calculations were updated accordingly.

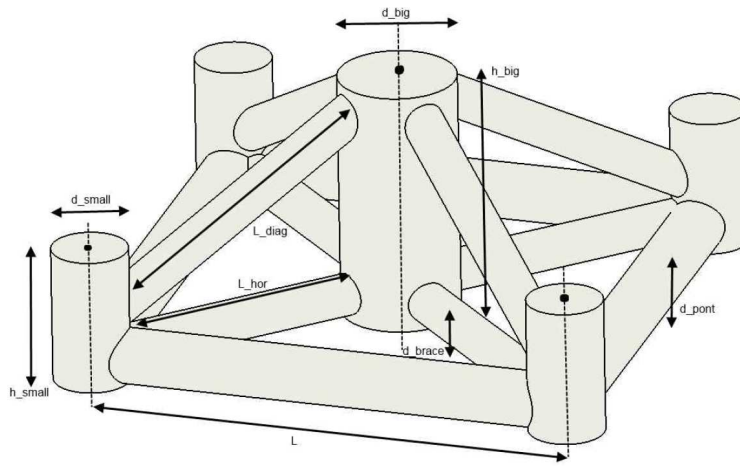


Figure 20: Improved mini-TLP geometry with parametric dimensions

Appendix C FE Pipe Model APDL

The first dimensions were calculated and used in a Finite Element model. This was done at first with use of PIPE289 elements. This resulted in a simple FE model with low calculation time and sufficient accuracy for design improvement. The tendons are modelled by LINK180 elements. At first a linear model was calculated and when the model was found reliable non-linear effects were taken into account.

Static: Buoyancy and gravity loading

At first the only loading applied on the structure was the calculated Buoyancy force and the gravity of the weight of the TLP itself. This was done in order to test if the structure was self-supporting, without external loads. The displacements were only in the upward directions and showed that the models behaviour is plausible.

Static: Extreme loading

Since the model behaved like it was supposed to, external loads were applied on the structure. These external loads were the governing extreme loads of the 6MW turbine Load report (ref. [6]). The first analysis showed immediately that insufficient buoyancy force was applied. This was expected since the complex 3D problem was simplified to a 2D problem which did not take in account all forces applied. This insufficient buoyancy force can be seen in Figure 21.

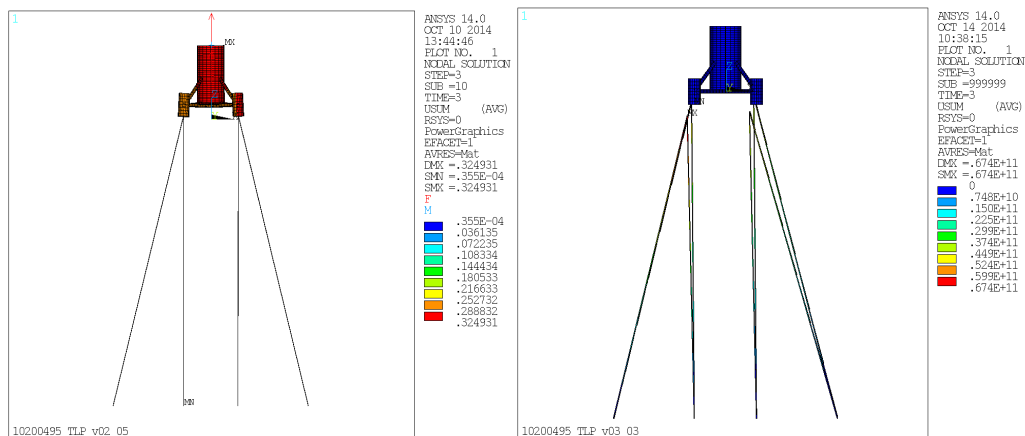


Figure 21: Buoyancy force only (left) and collapse of the system with external forces (right)

The buoyancy force was increased iteratively and the geometry adjusted accordingly, till acceptable displacements and stresses were present for the extreme loads. Also the geometry was limited in height to improve producibility. This led to a more sensible and elegant design with good properties as can be seen in Figure 22.

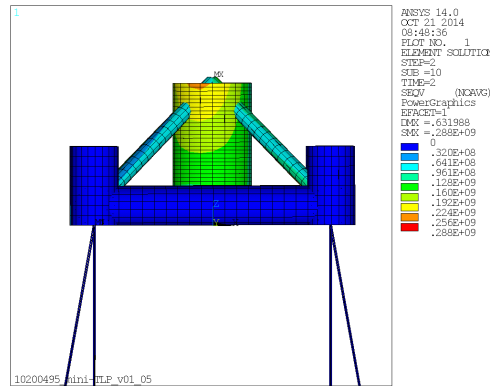


Figure 22: Equivalent stress of the improved design for the governing load case

Static: Stability analysis

The stability of the structure was tested to see when tension was lost or when the structure collapsed. This was done by increasing the forces of the extreme loads till tension was lost in one of the cables. The structure became unstable for several times the extreme load case. The analysis showed that the structure was quite robust and it did not require improvements for stability.

Static: Stiffness analysis

The stiffness of the structure was analysed and tested for a linear curve. The stiffness was calculated by applying a unit force and analysing the displacement or rotation and using the equations:

$$K_x = \frac{F_x}{u_x} \text{ and } C_z = \frac{M_z}{\theta_z}$$

The unit loads were varied in their amplitude and the stiffness was calculated for each of these unit loads. The analysis showed that the structure has a linear stiffness curve, as can be seen in Figure 23.

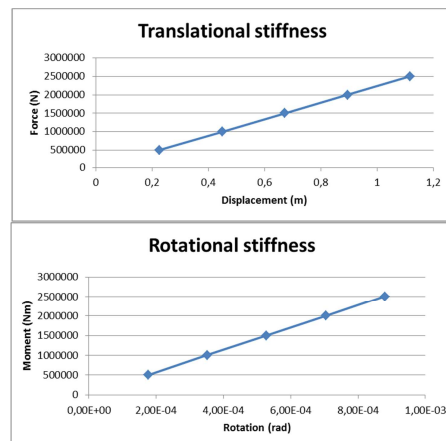


Figure 23: Stiffness curves for translational and rotational stiffness



Appendix D FE Shell Model APDL

A reliable model was set up with use of the PIPE elements. However this model did not give a lot of accuracy and the results of the displacement and stresses in the model were globally given. For the fatigue and ultimate strength analysis more accuracy was required and therefore SHELL281 elements were used to make a shell model. Shell elements were used since the model consists of relatively large components with thin walls, gave sufficient accuracy and an appropriate calculation time.

Static: Extreme loading

The extreme loads which were applied on the pipe model are also applied on the shell model. First, this was done to validate the model, to see if the results are similar to that of the pipe model. Second, as mentioned before the pipe model did not have a lot of accuracy and was used more in a global sense. The shell model revealed some weak spots in the structure which required some improvements. These were addressed with use of thicker walls, stiffer rings and flanges.

Static: Unit loading

The extreme loads revealed already some weak spots do to ultimate strength, which were then addressed. However, the structure must also to be tested for fatigue strength. This was done with use of the MECAL program ProDurA® version 2.11.0, but this required unit stresses to be calculated. Therefore unit loads were applied in order to retrieve these unit stresses. With use of ProDura a few additional weak spots were discovered and adjustments to the structure were made.

Static: Stability analysis

Also the shell structure was analysed for displacement stability. The criterion was based on the load factor required to make the tendons slack. Again, the analysis showed no problems with the stability.

Buckling: Linear stability analysis

Beside the displacement stability, the structure was also analysed for buckling, with a linear buckling stability analysis. The structure showed high safety factors, thus not requiring any action regarding buckling stability.



Appendix E FE model input

In this appendix the element types, material properties and section types are listed that are used in the TLP foundation FE component model. Please be referred to Appendix B, Appendix C and Appendix D for more information on the realization of the TLP geometry.

The element types, material properties and section properties are listed in Table 15, Table 16 and Table 17 respectively.

Table 15: FE model element types

ELEMENT TYPE	180 IS LINK180	3-D TENSION-ONLY SPAR
KEYOPT(1- 6)=	0 0	1 0 0 0
KEYOPT(7-12)=	0 0	0 0 0 0
KEYOPT(13-18)=	0 0	0 0 0 0
ELEMENT TYPE	281 IS SHELL281	8-NODE SHELL
KEYOPT(1- 6)=	0 0	0 0 0 0
KEYOPT(7-12)=	0 0	0 0 0 0
KEYOPT(13-18)=	0 0	0 0 0 0
ELEMENT TYPE	21 IS MASS21	STRUCTURAL MASS
KEYOPT(1- 6)=	0 0	0 0 0 0
KEYOPT(7-12)=	0 0	0 0 0 0
KEYOPT(13-18)=	0 0	0 0 0 0
ELEMENT TYPE	188 IS BEAM188	3-D 2-NODE BEAM
KEYOPT(1- 6)=	0 0	0 0 0 0
KEYOPT(7-12)=	0 0	0 0 0 0
KEYOPT(13-18)=	0 0	0 0 0 0

Table 16: FE model material properties

MATERIAL NUMBER	1
TEMP	EX
	0.2100000E+12
TEMP	NUXY
	0.3000000
TEMP	DENS
	7850.000
TEMP	MU
	0.4000000
MATERIAL NUMBER	188
TEMP	EX
	0.2100000E+12
TEMP	NUXY
	0.3000000
TEMP	DENS
	0.1000000
MATERIAL NUMBER	180
TEMP	EX
	0.1950000E+12
TEMP	NUXY
	0.3000000
TEMP	DENS
	5500.000



Table 17: FE model section properties

ON ID NUMBER	1			
INPUT SECTION TYPE		SHELL		
INPUT SHELL SECTION NAME		bs1		
Shell Section ID=	1	Number of layers=	1	Total Thickness= 0.030000
INPUT SECTION ID NUMBER	2			
INPUT SECTION TYPE		SHELL		
INPUT SHELL SECTION NAME		bs2		
Shell Section ID=	2	Number of layers=	1	Total Thickness= 0.030000
INPUT SECTION ID NUMBER	3			
INPUT SECTION TYPE		SHELL		
INPUT SHELL SECTION NAME		bs3		
Shell Section ID=	3	Number of layers=	1	Total Thickness= 0.024000
INPUT SECTION ID NUMBER	4			
INPUT SECTION TYPE		SHELL		
INPUT SHELL SECTION NAME		bs4		
Shell Section ID=	4	Number of layers=	1	Total Thickness= 0.024000
INPUT SECTION ID NUMBER	5			
INPUT SECTION TYPE		LINK		
INPUT LINK SECTION NAME		ls5		
Area		= 1.84050E-02		
INPUT SECTION ID NUMBER	6			
INPUT SECTION TYPE		SHELL		
INPUT SHELL SECTION NAME		bs6		
Shell Section ID=	6	Number of layers=	1	Total Thickness= 0.050000
INPUT SECTION ID NUMBER	7			
INPUT SECTION TYPE		SHELL		
INPUT SHELL SECTION NAME		bs7		
Shell Section ID=	7	Number of layers=	1	Total Thickness= 0.200000

Appendix F FE model plots

In this appendix the FE model plots are presented.

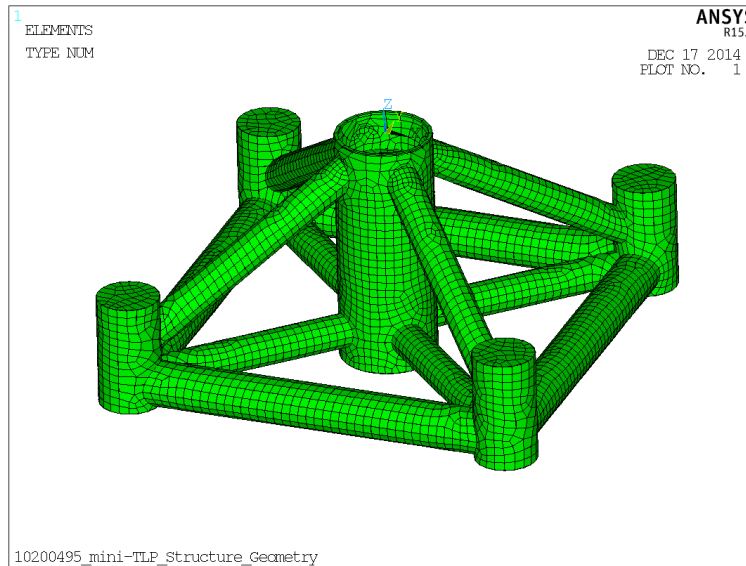


Figure 24: TLP structure model mesh

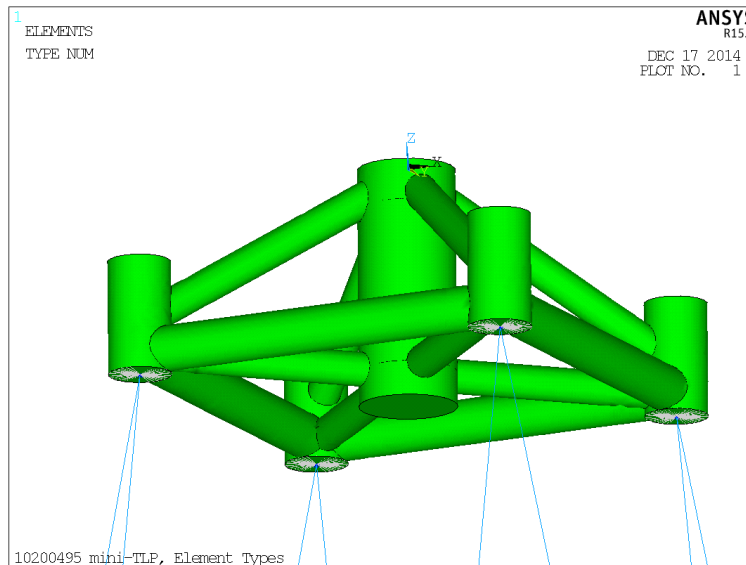


Figure 25: Model element types (blue = LINK180, grey = BEAM188 and green = SHELL281)

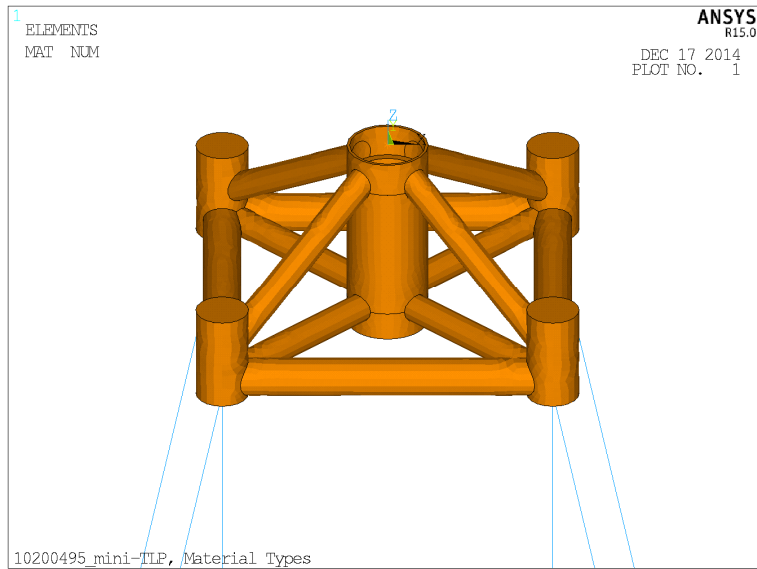


Figure 26: Model materials (orange = steel and blue = steel strand wire rope)

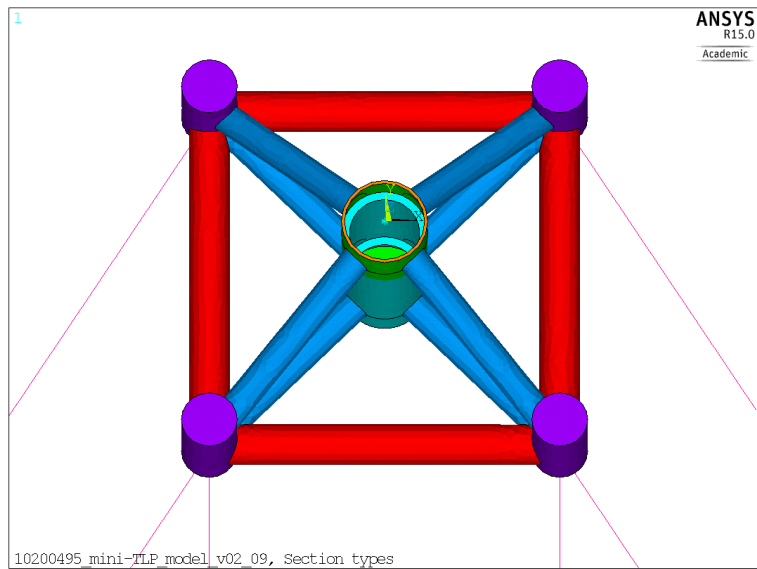


Figure 27: Model section types (purple = bs1, turquoise = bs2, red = bs3, blue = bs4, pink = ls5, green = bs6 and orange = bs7)

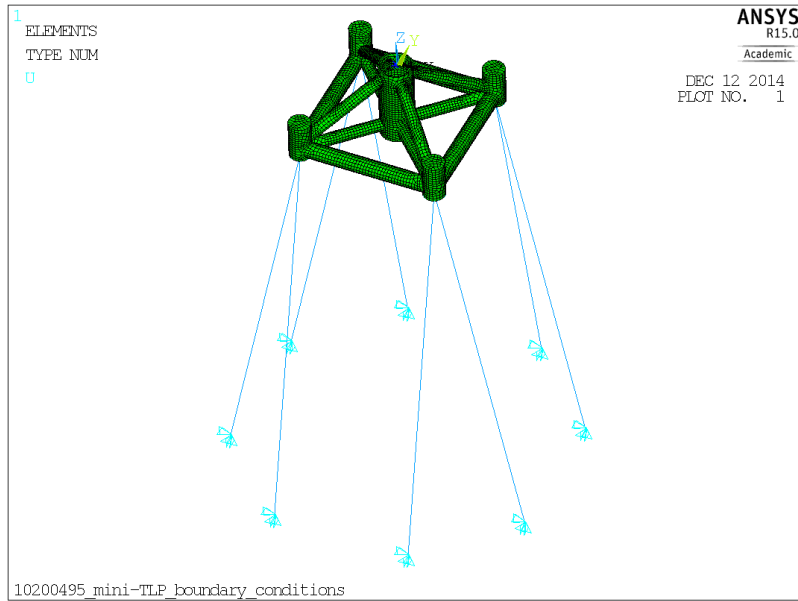


Figure 28: Model boundary conditions at the bottom nodes of the tendons

Appendix G FE calculation result plot

This appendix presents displacement and equivalent stress plots of the TLP structure for the unit force and moment load cases. Due to symmetry of the structure the unit load case Fx and Fy give similar results. The same holds for unit load case Mx and My. Therefore, the plots for the Fy and My load case are not shown. The displacements are given in [m] and the stresses in [Pa].

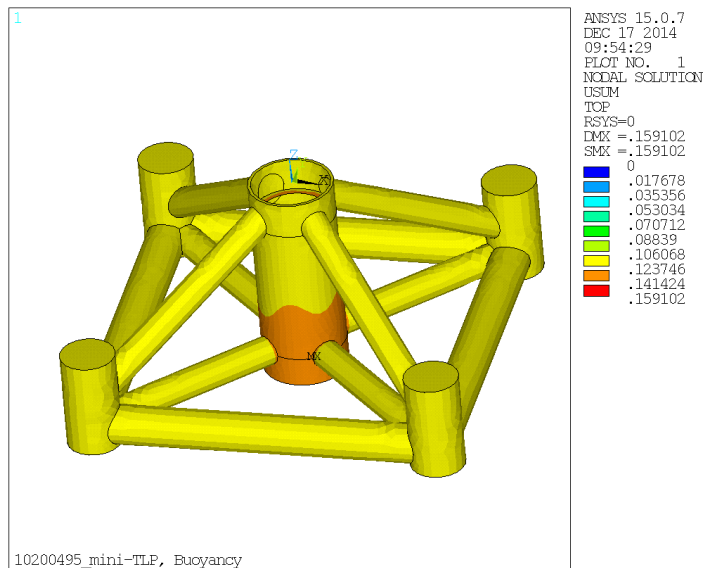


Figure 29: TLP structure displacements, Buoyancy load case

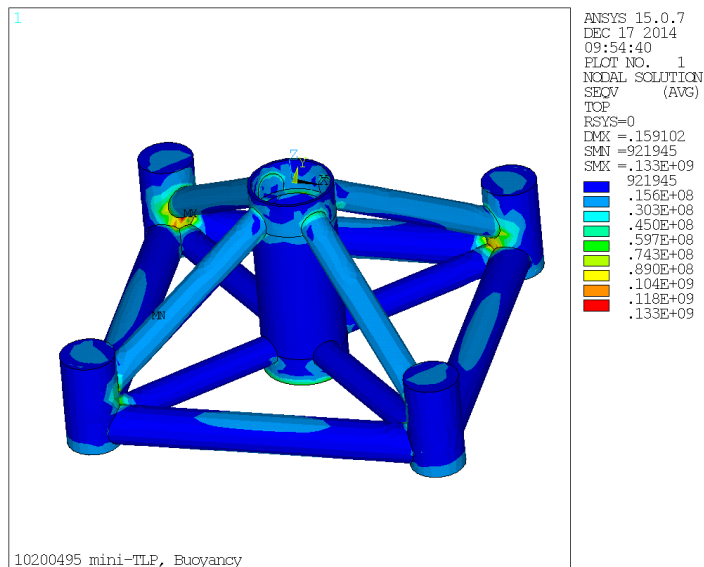


Figure 30: TLP structure equivalent stress, Buoyancy load case

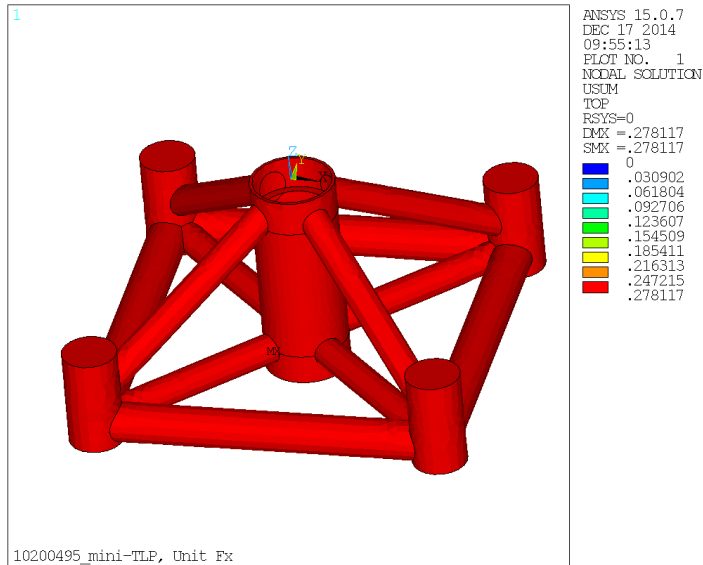


Figure 31: TLP structure displacements, Fx unit load case

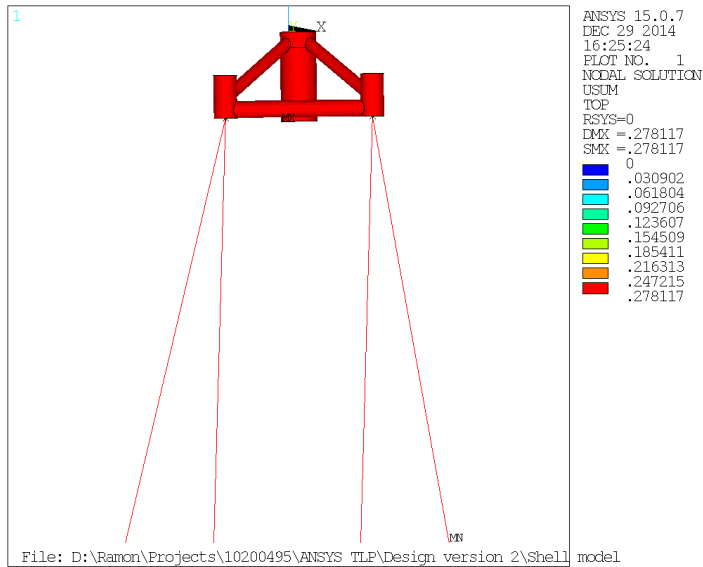


Figure 32: TLP displacements, Fx unit load case

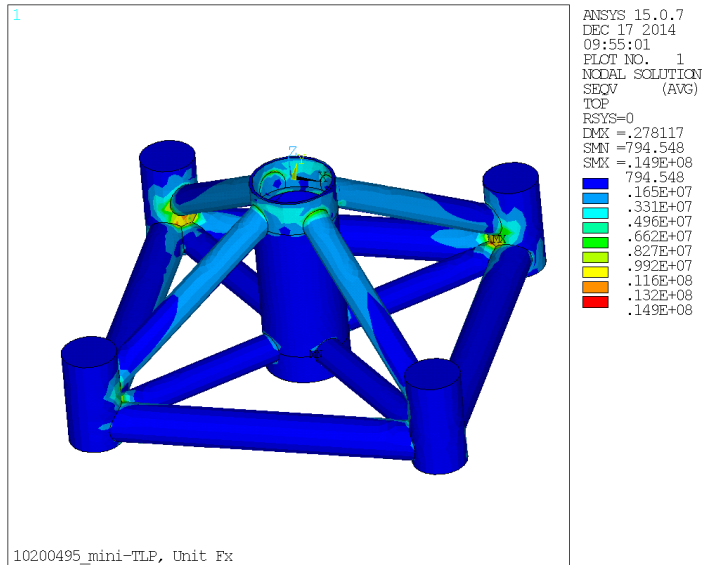


Figure 33: TLP structure equivalent stress, Fx unit load case

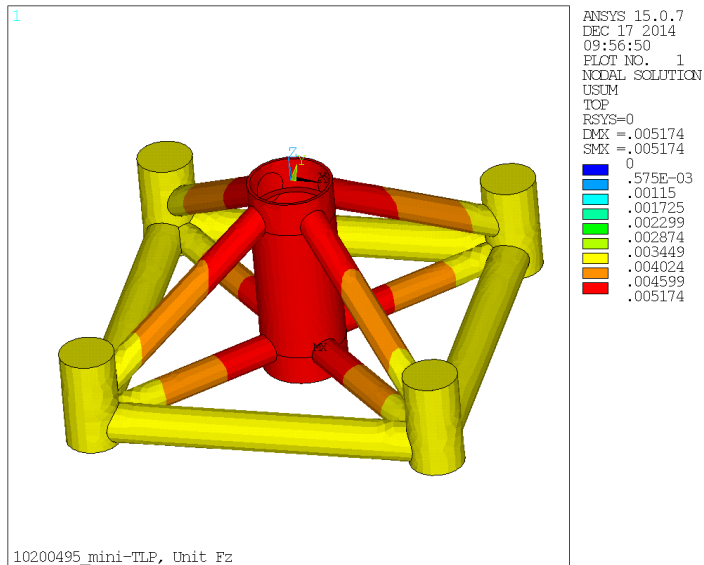


Figure 34: TLP structure displacements, Fz unit load case

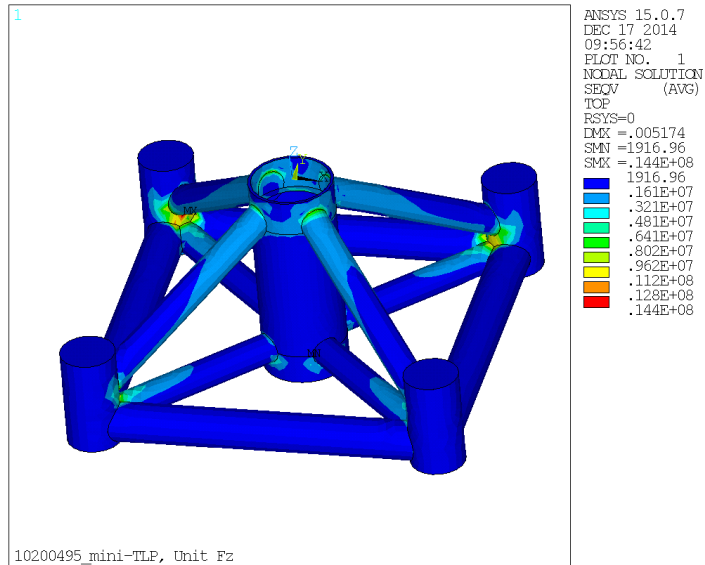


Figure 35: TLP structure equivalent stress, Fz unit load case

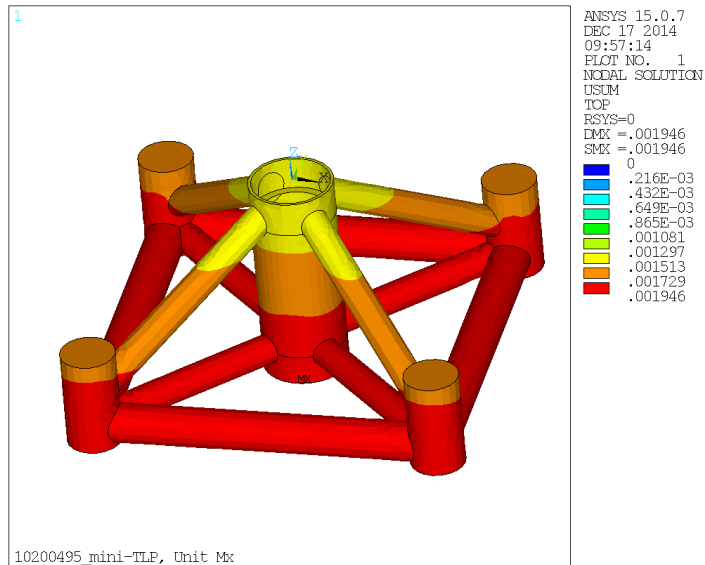


Figure 36: TLP structure displacements, Mx unit load case

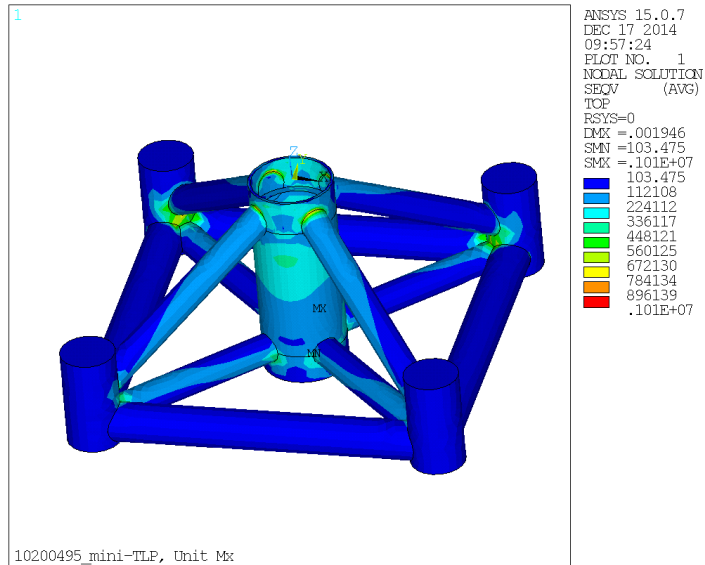


Figure 37: TLP structure equivalent stress, Mx unit load case

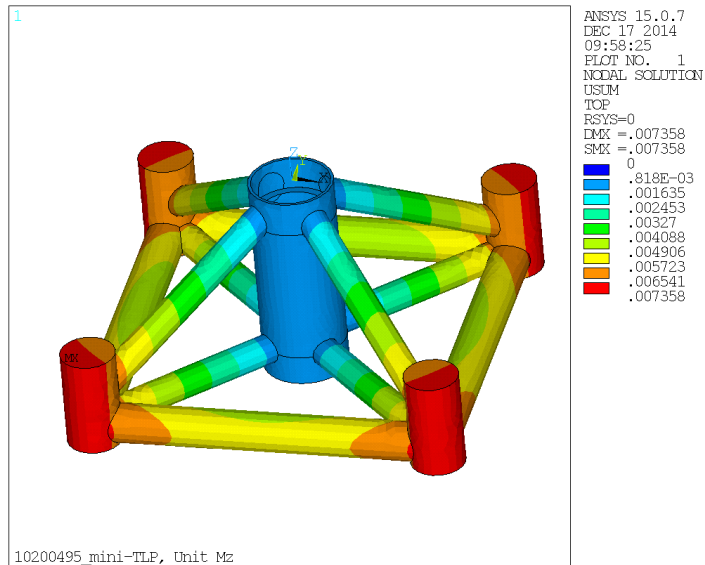


Figure 38: TLP structure displacements, Mz unit load case

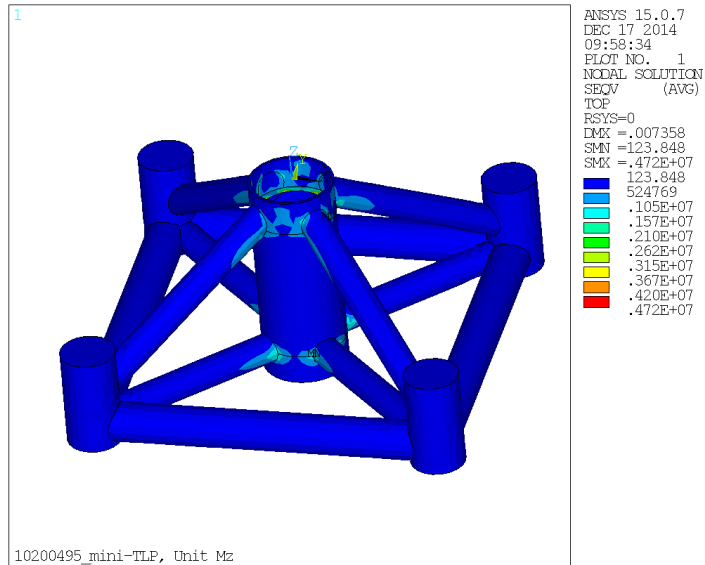


Figure 39: TLP structure equivalent stress, Mz unit load case



Appendix H Ocean wave frequencies

For determining the frequencies of ocean waves the DNV recommended practice DNV-RP-C205 is used (ref. [7]). Ocean waves are random; however, they can be split in several sinusoidal waves. For fully developed ocean waves, the waves are distributed according to the Pierson-Moskowitz spectrum. The Pierson-Moskowitz spectrum is defined as a function of the wave frequency. This function uses the significant wave height H_s and the peak period T_p (sometimes also given in zero-up crossing period T_z) to give the spectrum of waves of a certain sea state, as can be seen in the equation:

$$S_{PM}(\omega) = \frac{5}{16} \cdot H_s^2 \omega_p^4 \cdot \omega^{-5} \cdot e^{-\frac{5}{4} \left(\frac{\omega}{\omega_p}\right)^4} \quad \text{with } \omega_p = \frac{2\pi}{T_p}$$

The significant wave height and the peak period are independent variables, which have a certain chance of occurring in a predefined time period. Their change of occurrence is given in a scatter diagram. Every bin in the scatter diagram represents a different sea state with different PSD distribution.

Two scatter diagrams are available: one for the North Atlantic Ocean and one for the world-wide trade. An example of a scatter diagram can be seen in Figure 40.

T_p (s)	3.5	4.5	5.5	6.5	7.5	8.5	9.5	10.5	11.5	12.5	13.5	14.5	15.5	16.5	17.5	Sum
1.0	311	2734	6402	7132	5071	2711	1202	470	169	57	19	6	2	1	0	24287
2.0	20	764	4453	8841	9045	6020	3000	1225	435	140	42	12	3	1	0	34001
3.0	0	57	902	3474	5549	4973	3004	1377	518	169	50	14	4	1	0	20092
4.0	0	4	150	1007	2401	2881	2156	1154	485	171	53	15	4	1	0	10482
5.0	0	0	25	258	859	1338	1230	776	372	146	49	15	4	1	0	5073
6.0	0	0	4	63	277	540	597	440	240	105	39	13	4	1	0	2323
7.0	0	0	1	15	84	198	258	219	136	66	27	10	3	1	0	1018
8.0	0	0	0	4	25	69	103	99	69	37	17	6	2	1	0	432
9.0	0	0	0	1	7	23	39	42	32	19	9	4	1	1	0	178
10.0	0	0	0	0	2	7	14	16	14	9	5	2	1	0	0	70
11.0	0	0	0	0	1	2	5	6	6	4	2	1	1	0	0	28
12.0	0	0	0	0	0	1	2	2	2	2	1	1	0	0	0	11
13.0	0	0	0	0	0	0	1	1	1	1	0	0	0	0	0	4
14.0	0	0	0	0	0	0	0	0	1	0	0	0	0	0	0	1
Sum	331	3559	11937	20795	23321	18763	11611	5827	2489	926	313	99	29	9	0	100000

Figure 40: Scatter diagram for the world-wide trade (ref. [7])

Several values will be the input for the Pierson-Moskowitz distribution in order to see in which frequency range the waves occur. These distributions are shown in Figure 41.

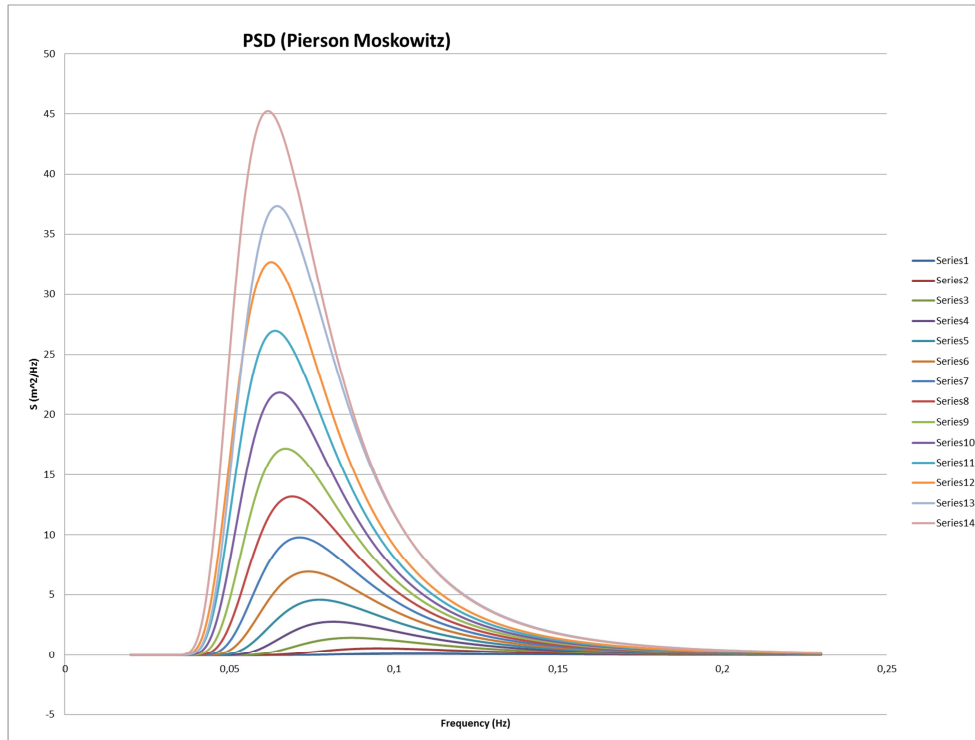


Figure 41: Pierson Moskowitz spectra for several ocean conditions

Appendix I Mode shapes

In this appendix the mode shapes of the modal analysis are presented. The frequency is given in [Hz].

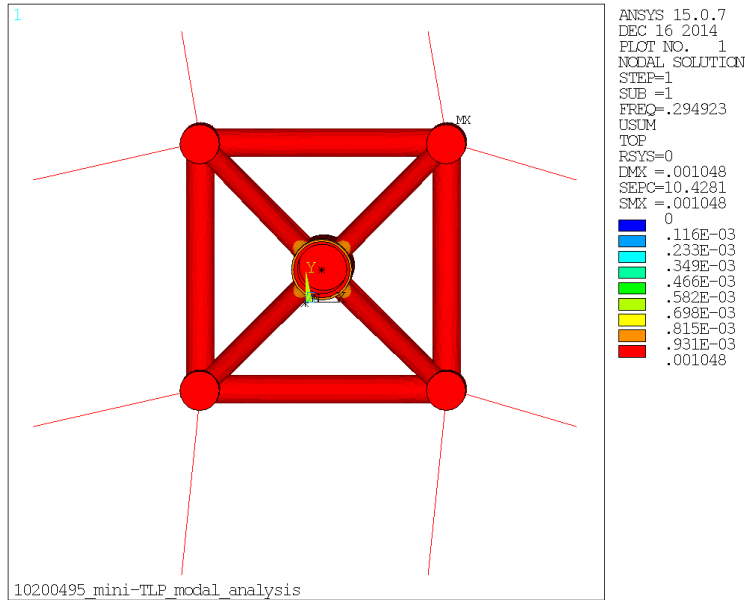


Figure 42: TLP foundation, mode shape 1

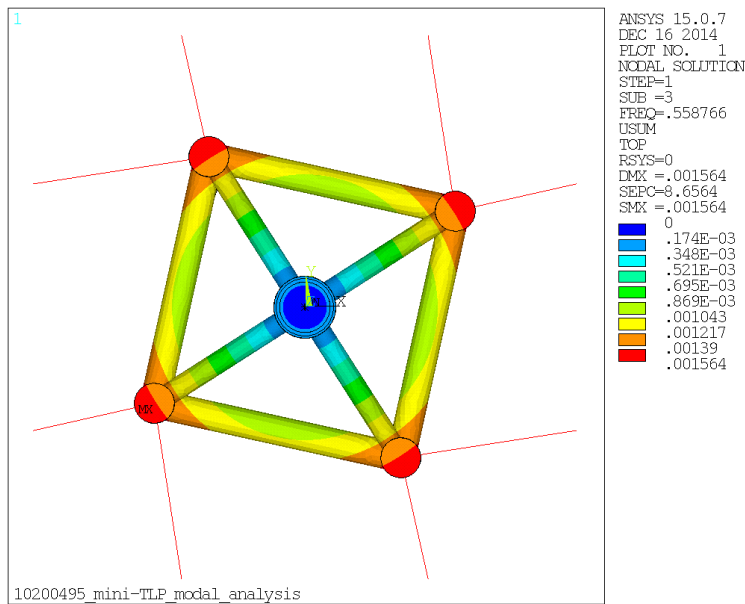


Figure 43: TLP foundation, mode shape 2

Appendix J Tendon tension results

This appendix presents axial stress of the tendons and the displacement of the TLP for the applied load cases in the stability analysis. The stresses are given in [Pa] and the displacements in [m].

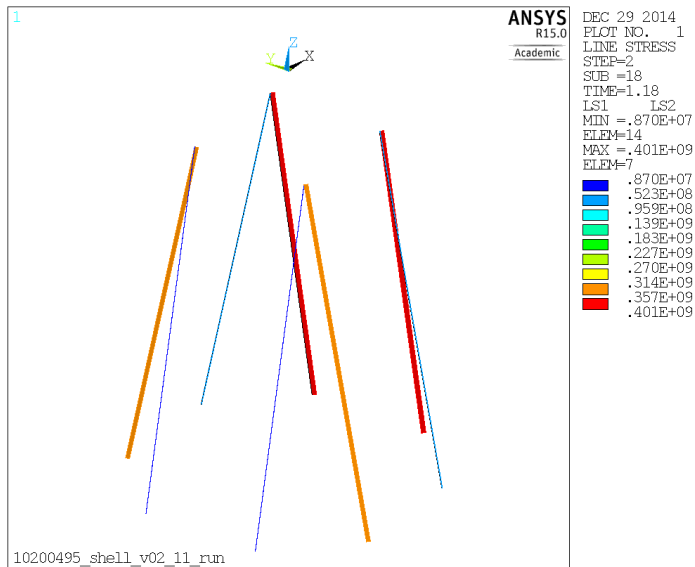


Figure 44: Axial stress of the tendons for load case 1 (factor 1.8)

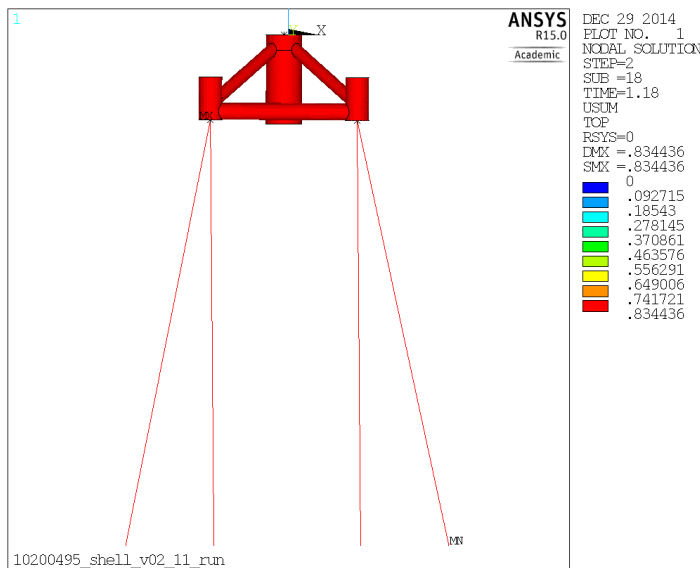


Figure 45: Total displacement of the TLP for load case 1 (factor 1.8)

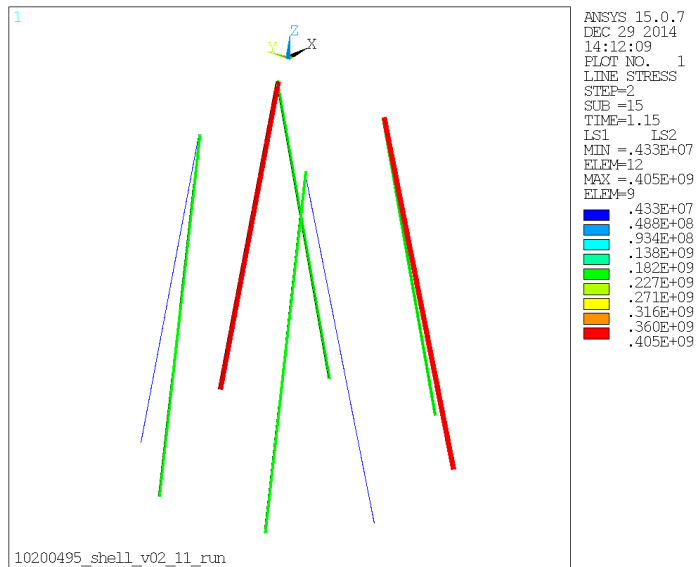


Figure 46: Axial stress of the tendons for load case 2 (factor 1.5)

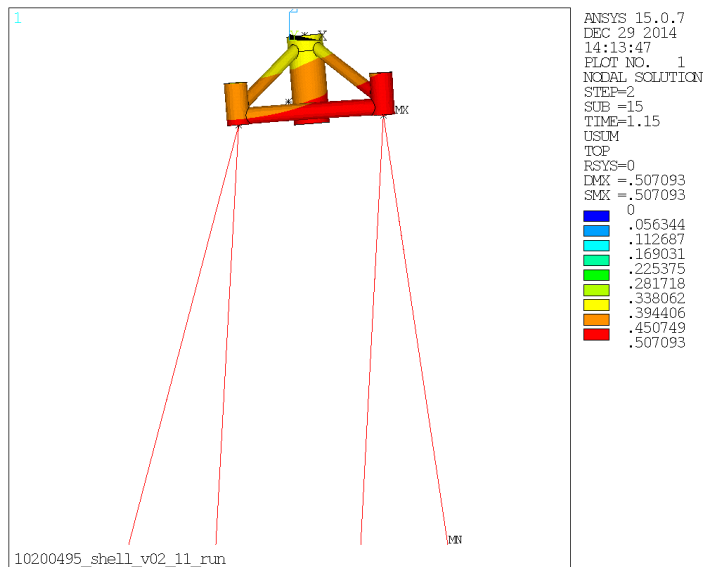


Figure 47: Total displacement of the TLP for load case 2 (factor 1.5)

Appendix K Buckling stability results

In this appendix the results of the linear buckling stability analysis are presented for the four lowest load factors as can be found in section 6.2.2.

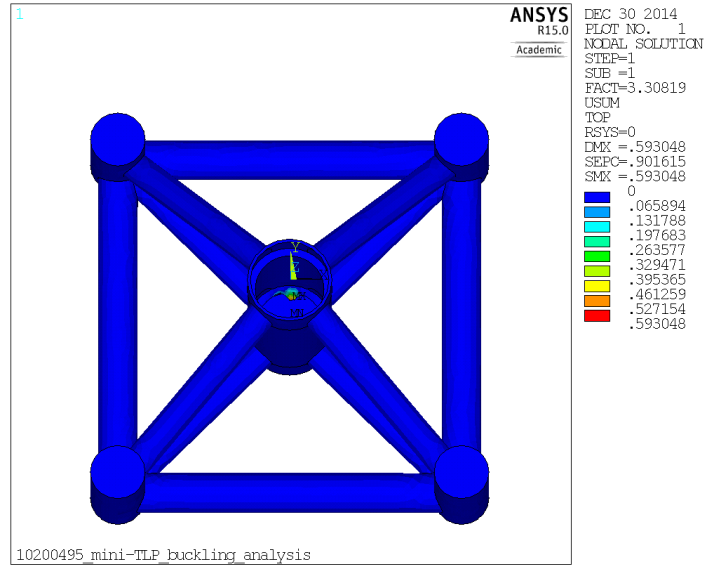


Figure 48: TLP structure, first buckling mode (stiffener ring)

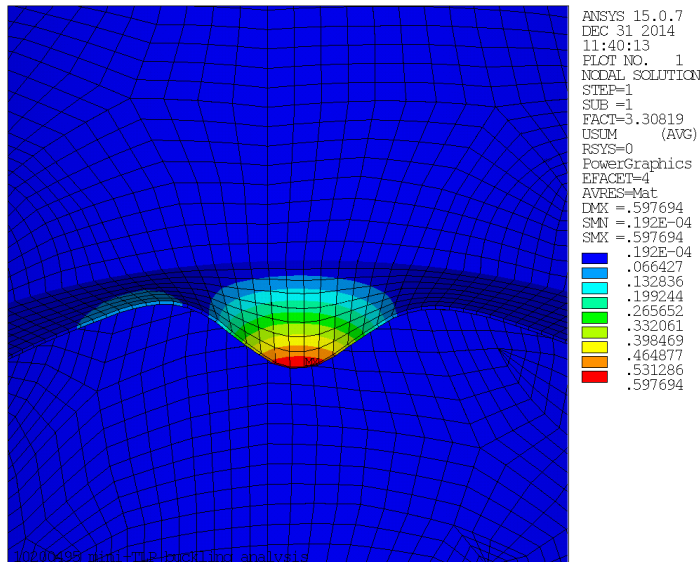


Figure 49: TLP structure, cross section view of first buckling mode

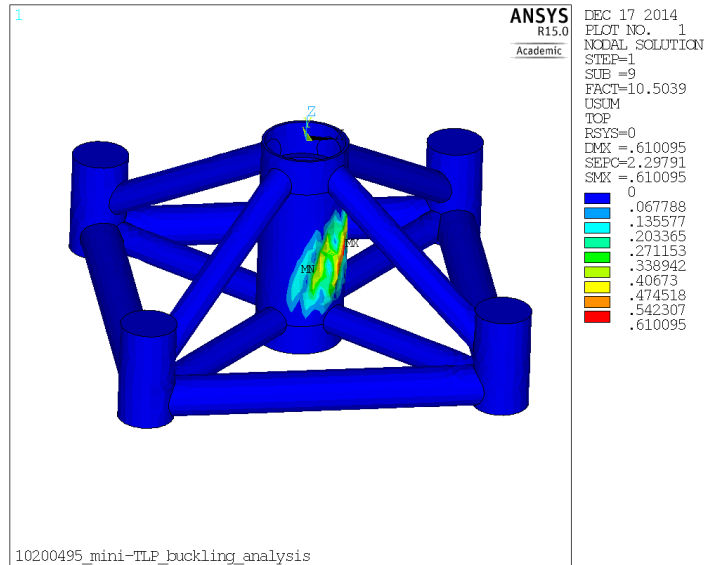


Figure 50: TLP structure, first tubular buckling mode

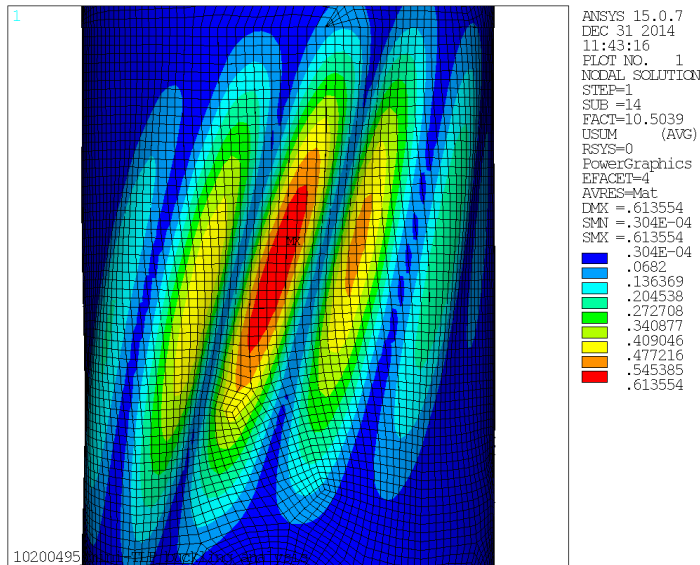


Figure 51: TLP structure, close up first tubular buckling mode

Report by:
Ramon Mertens, MECAL,
Enschede, the Netherlands

Commissioner:
MECAL Wind Turbine Design B.V.
Enschede, the Netherlands





Appendix L Equivalent load ranges

In this appendix the equivalent load ranges of top centre force, moment and acceleration load components are listed, as calculated by rainflow counting of the fatigue loads (ref. [6]), using ProDurA®.

Equivalent load ranges

--



Appendix M Extreme loads

This appendix presents the extreme load cases (ref.[6]), for which the ultimate strength of the TLP structure is calculated.

Extreme load cases

			TowerbottomMxCB	TowerbottomMyCB	TowerbottomMxyCB	TowerbottomMzCB	TowerbottomFxCB	TowerbottomFyCB	TowerbottomFxyCB	TowerbottomFzCB
			FL [Nm]	FL [Nm]	FL [Nm]	FL [Nm]	F [N]	F [N]	F [N]	F [N]
TowerbottomMxCB	MAX	ua62_42.5_709ea								
TowerbottomMxCB	MIN	ua62_42.5_414ka								
TowerbottomMyCB	MAX	un15_3abd								
TowerbottomMyCB	MIN	un15_2adc								
TowerbottomMxyCB	MAX	un15_2adc								
TowerbottomMxyCB	MIN	f64_27_204c								
TowerbottomMzCB	MAX	ua22a_2l								
TowerbottomMzCB	MIN	ua22a_2f								
TowerbottomFxCB	MAX	un15_2acb								
TowerbottomFxCB	MIN	un15_2adc								
TowerbottomFyCB	MAX	ua62_42.5_414ka								
TowerbottomFyCB	MIN	ua62_42.5_709ea								
TowerbottomFxyCB	MAX	ue61_42.5_961bc								
TowerbottomFxyCB	MIN	f64_2_40b								
TowerbottomFzCB	MAX	f23b_25_52								
TowerbottomFzCB	MIN	UT81a_1aec								

Appendix N Fatigue strength results

This appendix presents the fatigue strength results for the TLP structure in the form of fatigue SRF plots (SRF_{fat}). The plots show the TLP structure regions with the lowest fatigue strength. The SRF_{fat} values in the grey-coloured areas are higher than the maximum contour value mentioned in the legend next to each plot.

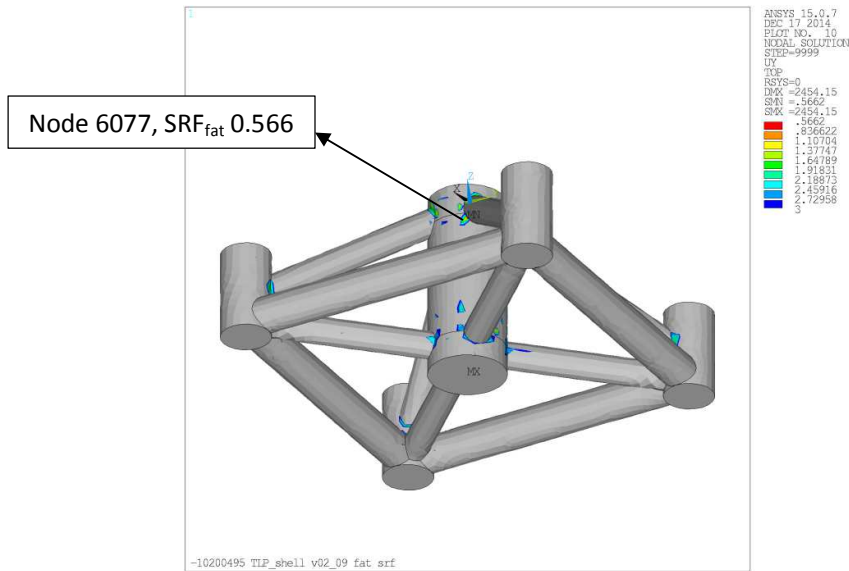


Figure 52: TLP structure fatigue SRF plot

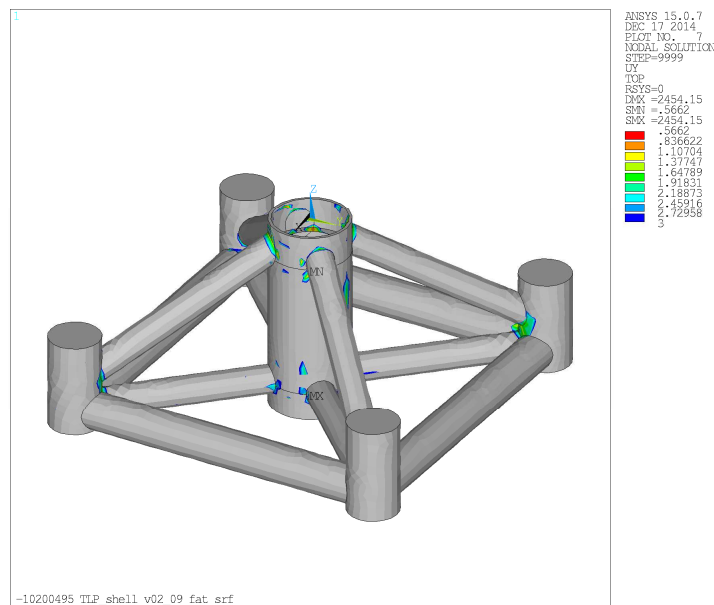


Figure 53: TLP structure fatigue SRF plot

©MECAL 2014. All right reserved.

Reproduction in whole or in parts is prohibited without the prior written consent of MECAL.

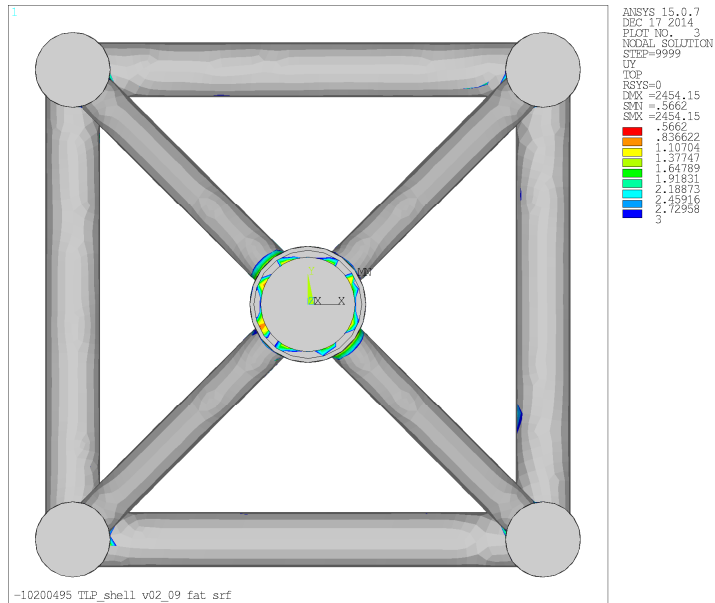


Figure 54: TLP structure fatigue SRF plot

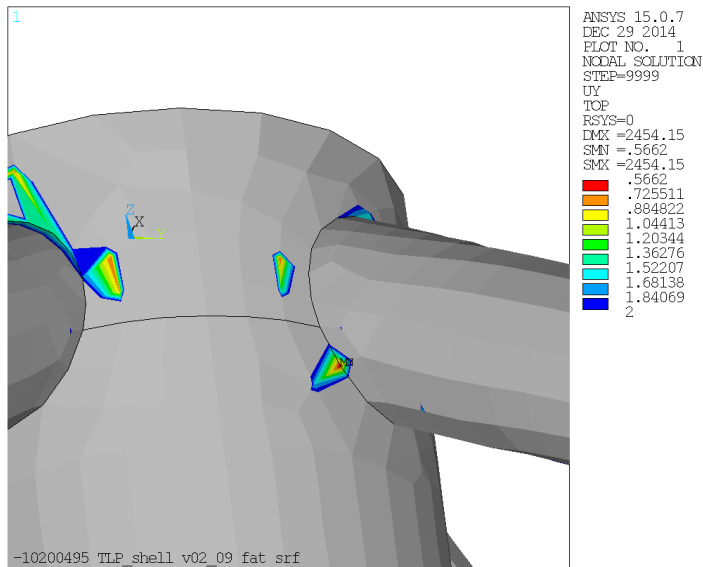


Figure 55: TLP structure fatigue SRF plot, close up



Appendix O Fatigue strength calculation output

```

Mecal Wind Turbine Design, ProDurA v2.11.0 Fatigue damage output 16-12-2014
=====
General calculation settings, applicable to all spots
-----
Admissible damage                : 1.00
Load factor gammaF               : 1.20
Material factor gammaM           : 1.10
Consequence of failure factor gammaN : 1.15
User factor l                    : 1.00

-----
S/N curve settings
-----
Safety factors standard          : IEC61400-1
SNCurve method                  : FAT (custom SN curve)
Right side slope method         : user defined

-----
S/N curve (all R)
-----
ds2 [MPa]                       : 71.0
Left side slope                  : 3.0
Right side slope                 : 5.0
Knee number n2                  : 5.000E+06
Cut off [-]                     : 0.00

Mecal Wind Turbine Design, ProDurA v2.11.0 Fatigue damage output 16-12-2014
=====
Node number: 6077

Stress reserve factor: 0.57
Damage (SRF=1)           : 1.712E+01

Calculation (damage threshold for print out = 0.005)
-----
      smeani      dsi      ni      dami
-----
0.0000E+00      4.6332E+01      1.7503E+06      0.020
0.0000E+00      4.5458E+01      5.5225E+06      0.056
0.0000E+00      4.4584E+01      1.0439E+07      0.096
0.0000E+00      4.3709E+01      1.3801E+07      0.115
0.0000E+00      4.2835E+01      1.2797E+07      0.096
0.0000E+00      4.1961E+01      9.4421E+06      0.064
0.0000E+00      4.1087E+01      6.8649E+06      0.042
0.0000E+00      4.0213E+01      5.8384E+06      0.032
0.0000E+00      3.9338E+01      5.2034E+06      0.026
0.0000E+00      3.8464E+01      4.2621E+06      0.019
0.0000E+00      3.7590E+01      2.8985E+06      0.011
0.0000E+00      3.6716E+01      1.9160E+06      0.007
-9.0996E-01      4.8080E+01      1.0026E+06      0.013
-9.0996E-01      4.7206E+01      2.4947E+06      0.031
-9.0996E-01      4.6332E+01      4.5491E+06      0.051
-9.0996E-01      4.5458E+01      6.0842E+06      0.062
-9.0996E-01      4.4584E+01      6.4428E+06      0.059
-9.0996E-01      4.3709E+01      5.7343E+06      0.048
-9.0996E-01      4.2835E+01      4.5803E+06      0.035
-9.0996E-01      4.1961E+01      3.7675E+06      0.026
-9.0996E-01      4.1087E+01      2.9987E+06      0.018
-9.0996E-01      4.0213E+01      2.5158E+06      0.014
-9.0996E-01      3.9338E+01      1.9090E+06      0.009
-9.0996E-01      3.8464E+01      1.3017E+06      0.006
-----
                                1.1134E+09      1.003
-----

Linear spot unit stresses
Sensor      sxx      syy      szz      sxy      syz
61: Tower_bottom_Fx_CB      7.5518E+05      -1.3055E+06      -6.3998E+05      9.9090E+05      -2.7717E+05
62: Tower_bottom_Fy_CB      4.2845E+05      -7.8977E+05      -2.8721E+05      6.0515E+05      -2.3915E+04

```



63: Tower_bottom_Fz_CB	-8.8337E+05	5.9746E+05	1.5415E+05	-6.4901E+05	2.2078E+05
65: Tower_bottom_Mx_CB	-4.2988E+04	-6.2765E+04	1.7120E+04	1.2864E+04	4.5463E+04
66: Tower_bottom_My_CB	3.0347E+04	-2.9398E+04	-1.5925E+05	2.5147E+04	2.8885E+04
67: Tower_bottom_Mz_CB	9.0415E+04	-4.9150E+05	-3.4109E+05	2.9685E+05	7.9026E+03
	szz	gain			
	5.3767E+05	1.0000E-09			
	2.2480E+05	1.0000E-09			
	-3.7343E+05	1.0000E-09			
	-1.2627E+04	1.0000E-09			
	-4.4157E+03	1.0000E-09			
	1.1816E+05	1.0000E-09			

Appendix P Ultimate fatigue strength results

This appendix presents the ultimate fatigue strength results for the TLP structure in the form of ultimate fatigue SRF plots (SRF_{ultfat}). The plots show the TLP structure regions with the lowest ultimate fatigue strength. The SRF_{ultfat} values in the grey-coloured areas are higher than the maximum contour value mentioned in the legend next to each plot.

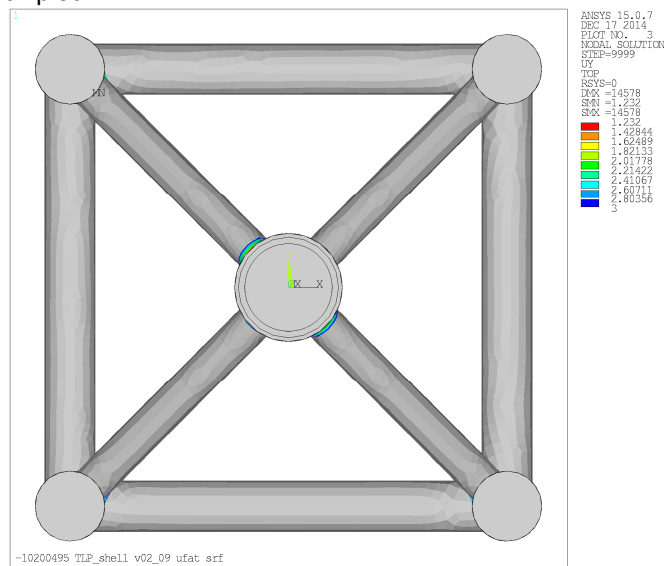


Figure 56: TLP structure ultimate fatigue SRF plot, top view

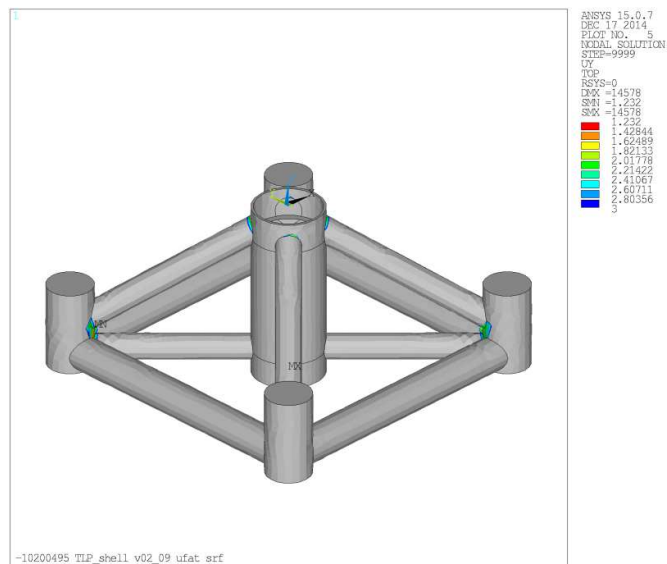


Figure 57: TLP structure ultimate fatigue SRF plot

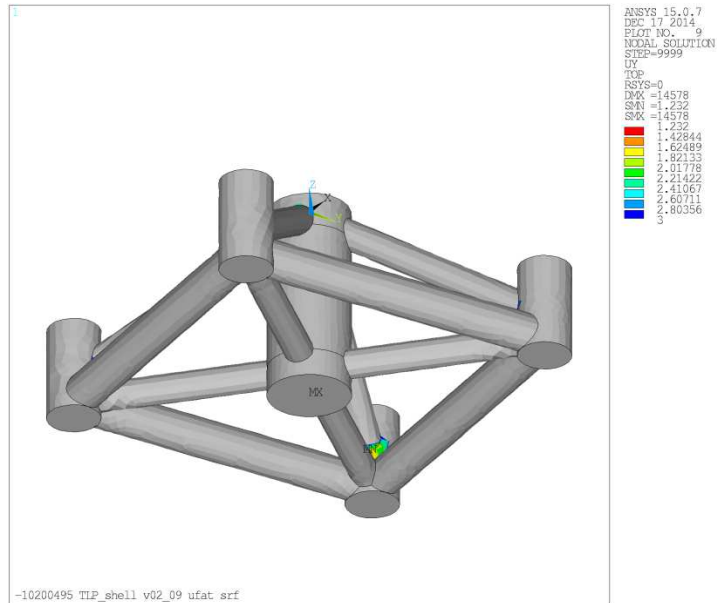


Figure 58: TLP structure ultimate fatigue SRF plot

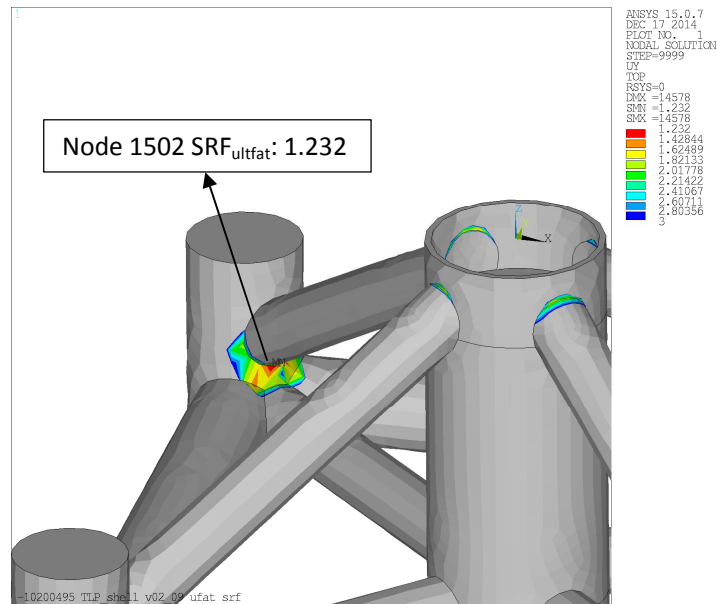


Figure 59: TLP structure ultimate fatigue SRF plot, close up



Appendix Q Ultimate fatigue strength calculation output

```

Mecal Wind Turbine Design, ProDurA v2.11.0 Ultimate strength output (fatigue files) 16-12-2014
=====
A. Main results
-----

Stress function
-----
Equivalent stress function      : Von Mises
Equivalent stress sign        : Extreme principal
Stress to use for SRF calculation : Absolute max

Load factor gammaF            : 1.00
Material factor gammaM        : 1.10
Consequence of failure factor gammaN : 1.15
Yield strength Re [MPa]      : 335
Stress concentration factor Kt : 1.00

Node number: 1502

Stress reserve factor: 1.23

Time signal values (note: the gain is already incorporated)
-----
Rank  Stress      SRF      ts -1      ts 61      ts 62      ts 63      ts 65
1     215.0      1.23    0.0000E+00 -5.0394E-07  7.4454E-07 -7.6591E-06 -5.4823E-05
2     214.2      1.24    0.0000E+00 -6.3999E-07  6.2498E-07 -7.5823E-06 -4.6869E-05
3     211.6      1.25    0.0000E+00 -6.0336E-07  6.0135E-07 -7.6261E-06 -4.5054E-05
4     210.7      1.26    0.0000E+00 -4.1312E-07  7.9027E-07 -7.5985E-06 -5.8133E-05
5     210.7      1.26    0.0000E+00 -6.4975E-07  5.3918E-07 -7.6597E-06 -4.0194E-05
6     209.4      1.26    0.0000E+00 -4.2247E-07  6.7019E-07 -7.6610E-06 -5.1035E-05
7     208.9      1.27    0.0000E+00 -6.0686E-07  5.6202E-07 -7.6056E-06 -4.2587E-05
8     207.3      1.28    0.0000E+00 -3.4058E-07  8.0447E-07 -7.6035E-06 -5.8454E-05
9     207.2      1.28    0.0000E+00 -3.1439E-07  8.5497E-07 -7.5900E-06 -6.1795E-05
10    207.2      1.28    0.0000E+00 -2.4765E-07  8.8011E-07 -7.6592E-06 -6.3774E-05

      ts 66      LineNr      File
-6.0350E-05      3148      fat821.dat
-6.8418E-05      2897      fat809.dat
-6.7152E-05      4448      fat641.dat
-5.3411E-05      5769      fat834.dat
-7.0412E-05      5771      fat833.dat
-5.9556E-05      11831     fat786.dat
-6.7022E-05      4615      fat797.dat
-4.9449E-05      3141      fat822.dat
-4.5863E-05      2899      fat810.dat
-4.3282E-05      9808      fat846.dat

File with spot unit stresses
D:\Ramon\Projects\10200494\ANSYS          TLP\Design          version          2\Shell          model\v02\v02_09
improved\7_strength\stresses.txt
Directory with load files
D:\Ramon\Projects\10200494\Loads&Calculations\XXXXX_6MW_loadset_V02\4_1_conversion_v02A\1_dat\fat\
File with sensor information
D:\Ramon\Projects\10200494\Loads&Calculations\XXXXX_6MW_loadset_V02\4_1_conversion_v02A\1_dat\sens_pd.txt
File with occurrence data
D:\Ramon\Projects\10200494\Loads&Calculations\XXXXX_6MW_loadset_V02\4_1_conversion_v02A\1_dat\occ_fat.txt

Use reduced loads data          : No, all loads data is used for the calculation
Number of load cases            : 993  NOTE: load cases with an occurrence >1

Linear spot unit stresses
Sensor          sxx          syy          szz          sxy          syz
61: Tower_bottom_Fx_CB      7.4878E+06      5.7194E+06      1.3704E+07      6.5030E+06      -1.0994E+05
62: Tower_bottom_Fy_CB     -7.6263E+06     -5.7945E+06     -1.3900E+07     -6.6467E+06      2.6835E+05
63: Tower_bottom_Fz_CB      8.0044E+06      6.0860E+06      1.4286E+07      7.1429E+06      -8.7608E+03
65: Tower_bottom_Mx_CB      4.3144E+05      3.1939E+05      7.5224E+05      3.7717E+05      -1.8912E+03
66: Tower_bottom_My_CB      4.1709E+05      3.2618E+05      7.6028E+05      3.7504E+05      -1.5529E+03
67: Tower_bottom_Mz_CB     -2.4783E+04     -6.4372E+03     -2.4123E+04     -1.1115E+04     -4.0873E+02

```

Report by:
Ramon Mertens, MECAL,
Enschede, the Netherlands

Commissioner:
MECAL Wind Turbine Design B.V.
Enschede, the Netherlands



sxz	gain
1.2151E+05	1.0000E-09
1.0552E+05	1.0000E-09
5.2089E+04	1.0000E-09
2.8885E+03	1.0000E-09
4.6857E+03	1.0000E-09
-3.4376E+03	1.0000E-09

Appendix R Ultimate strength results

This appendix presents the ultimate strength results for the TLP structure in the form of extreme SRF plots (SRF_{ext}). The plots show the TLP structure regions with the lowest ultimate strength. The SRF_{ext} values in the grey-coloured areas are higher than the maximum contour value mentioned in the legend next to each plot.

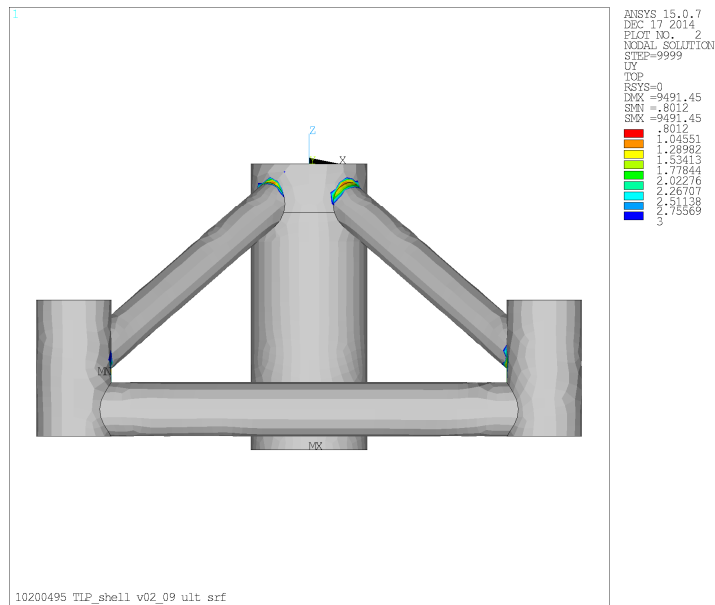


Figure 60: TLP structure ultimate SRF plot, side view

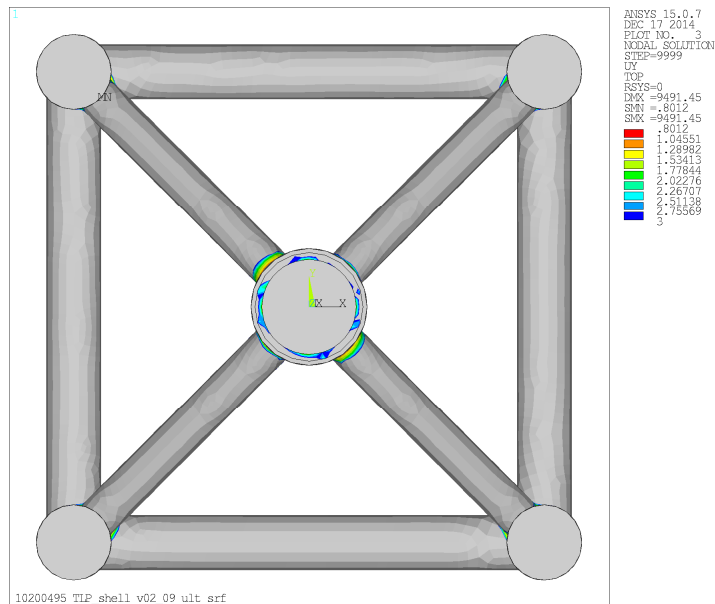


Figure 61: TLP structure ultimate SRF plot, top view

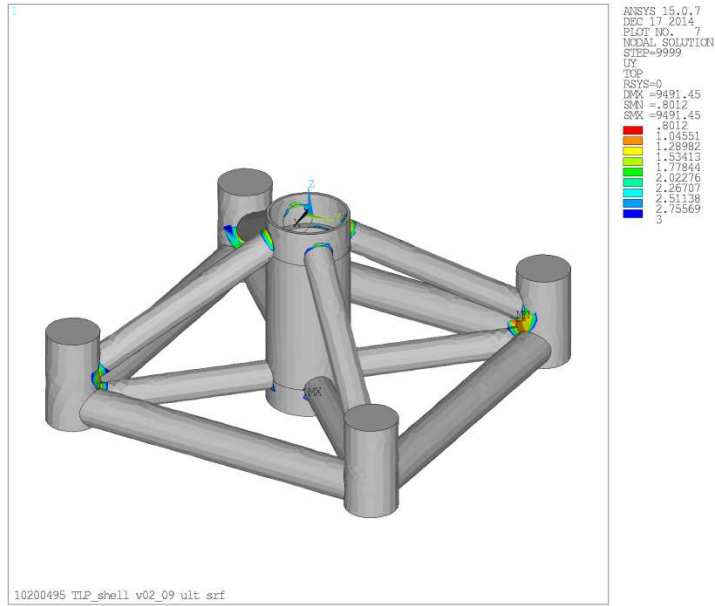


Figure 62: TLP structure ultimate SRF plot

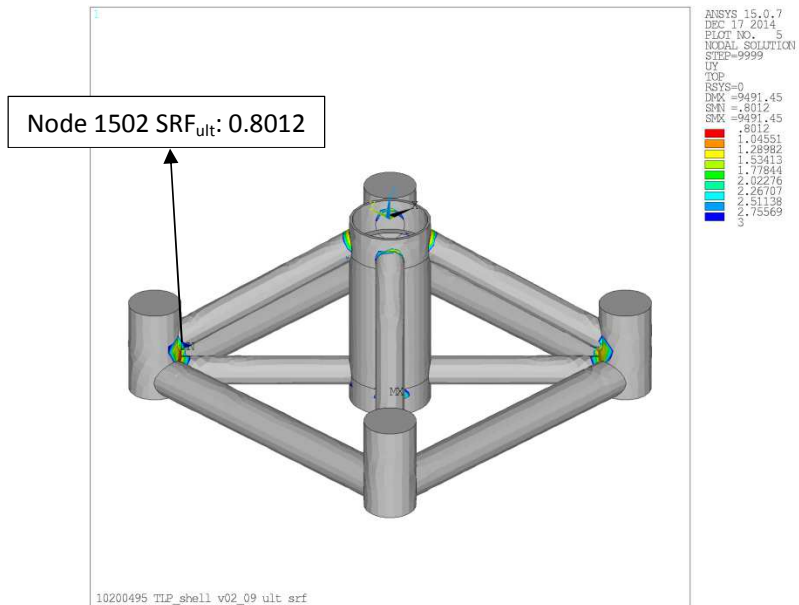


Figure 63: TLP structure ultimate SRF plot

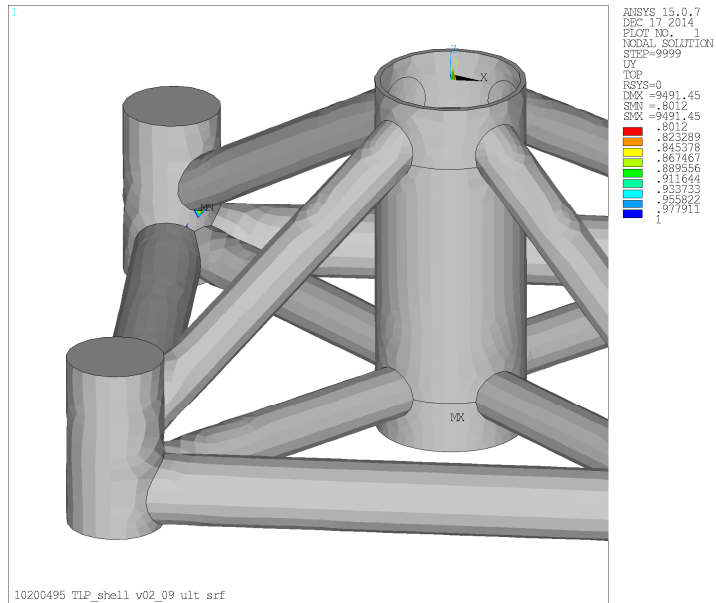


Figure 64: TLP structure ultimate SRF plot, close up

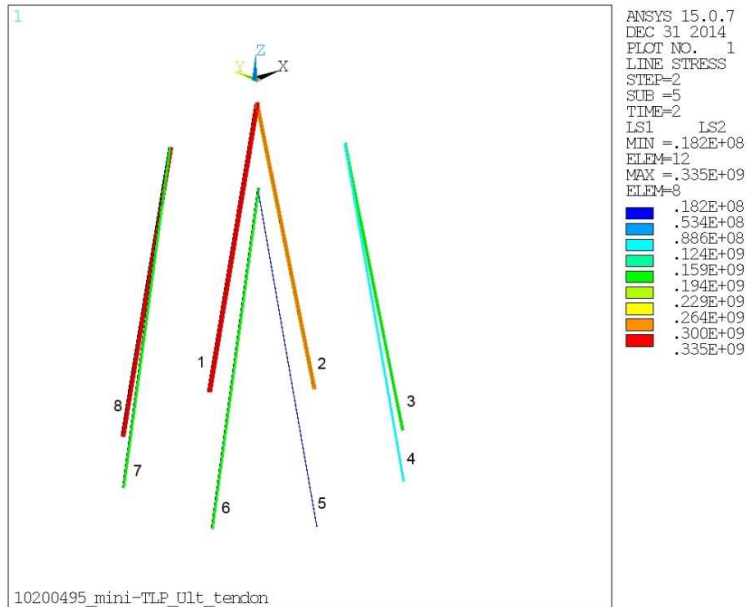


Figure 65: Axial stress in tendons, governing load case



Appendix S Ultimate strength calculation output

```

Mecal Wind Turbine Design, ProDurA v2.11.0 Ultimate strength output (extreme files) 16-12-2014
=====
Stress function
-----
Equivalent stress function      : Von Mises
Equivalent stress sign        : Extreme principal
Stress to use for SRF calculation : Absolute max

Load factor gammaF            : 1.20
Material factor gammaM        : 1.10
Consequence of failure factor gammaN : 1.00
Yield strength Re [MPa]       : 335
Stress concentration factor Kt : 1.00
-----

Mecal Wind Turbine Design, ProDurA v2.11.0 Ultimate strength output (extreme files) 16
=====
Node number: 1502

Stress reserve factor: 0.80

Time signal values (note: the gain is already incorporated)
-----
Rank  Stress      SRF      ts -1      ts 61      ts 62      ts 63      ts 65
  1    316.8      0.80    0.0000E+00 -1.7363E-06  1.2568E-07 -1.0542E-05 -9.7811E-06

      ts 66  LineNr  File
-1.7379E-04    98  ext_v02a.dat

File with spot unit stresses
D:\Ramon\Projects\10200494\ANSYS          TLP\Design          version          2\Shell          model\v02\v02_09
improved\7_strength\stresses.txt
Directory with load files
D:\Ramon\Projects\10200494\Loads&Calculations\XXXXXX_6MW_loadset_V02\4_1_conversion_v02A\1_dat\ext\
File with sensor information
D:\Ramon\Projects\10200494\Loads&Calculations\XXXXXX_6MW_loadset_V02\4_1_conversion_v02A\1_dat\sens_pd.txt
File with occurrence data
D:\Ramon\Projects\10200494\Loads&Calculations\XXXXXX_6MW_loadset_V02\4_1_conversion_v02A\1_dat\occ_ext.txt

Use reduced loads data          : No, all loads data is used for the calculation
Number of load cases            : 1  NOTE: load cases with an occurrence <=1

Linear spot unit stresses
Sensor                          sxx          syy          szz          sxy          syz
61: Tower_bottom_Fx_CB          7.4878E+06   5.7194E+06   1.3704E+07   6.5030E+06   -1.0994E+05
62: Tower_bottom_Fy_CB          -7.6263E+06  -5.7945E+06  -1.3900E+07  -6.6467E+06   2.6835E+05
63: Tower_bottom_Fz_CB          8.0044E+06   6.0860E+06   1.4286E+07   7.1429E+06   -8.7608E+03
65: Tower_bottom_Mx_CB          4.3144E+05   3.1939E+05   7.5224E+05   3.7717E+05   -1.8912E+03
66: Tower_bottom_My_CB          4.1709E+05   3.2618E+05   7.6028E+05   3.7504E+05   -1.5529E+03
67: Tower_bottom_Mz_CB          -2.4783E+04  -6.4372E+03  -2.4123E+04  -1.1115E+04   -4.0873E+02

      sxz          gain
1.2151E+05   1.0000E-09
1.0552E+05   1.0000E-09
5.2089E+04   1.0000E-09
2.8885E+03   1.0000E-09
4.6857E+03   1.0000E-09
-3.4376E+03   1.0000E-09

```



Appendix T Mathcad Calculation

```

c*****
c*** author:          rmer.
c*** checker:         xxxx
c*** file discription: Calculations on the TLP
c*** file name:       Preliminary calculations
c*** dimension:       length in [m]
c***                  mass in [kg]
c***                  time in [s]
c***                  copyright 2014 mecal bv
c*****

```

Parameters:

See figure

Geometry of the TLP:

d_small := 5.5	Diameter of small cylinder
h_small := 10	Height of small cylinder
d_big := 8.5	Diameter of main cylinder
h_big := 20	Height of main cylinder
t_cyl := 0.03	Thickness wall cylinders
L _{sv} := 34.5	Distance between small cylinders
d_pont := 4	Diameter of pontoon
t_pont := 0.024	Thickness wall pontoon
d_brace := 3	Diameter of brace
t_brace := 0.024	Thickness wall brace

Steel properties (St355):

ρ _{st} := 7850	Density of steel
E := 210·10 ⁹	Youngs modulus
ν := 0.3	Poisson ratio
σ := 335·10 ⁶	Yield stress

Other parameters:

ρ := 1025	Density of seawater
g := 9.81	Gravity
M _{wt} := 800000	Weight of the wind turbine

Bouyancy calculation of the cylinders:

Volume calculation:

Radius of cylinders:

$$r_{small} := \frac{d_{small}}{2} \quad r_{big} := \frac{d_{big}}{2} \quad r_{pont} := \frac{d_{pont}}{2} \quad r_{brace} := \frac{d_{brace}}{2}$$

Length of horizontal brace:

$$L_{hor} := \sqrt{2(0.5L)^2} - r_{big} - r_{small} \quad L_{hor} = 17.395$$

Angle of diagonal brace (in rad):

$$Angle := \text{atan} \left[\frac{h_{big} - 1 - r_{pont}}{\sqrt{2(0.5L)^2}} \right] \quad Angle = 0.609$$

Length of diagonal brace:

$$L_{diag} := \sqrt{2(0.5L)^2 + (h_{big} - 1 - r_{pont})^2} - [\cos(Angle) \cdot (r_{big} + r_{small})] \quad L_{diag} = 23.991$$

Volume of small cylinder:

$$V_{small} := \pi r_{small}^2 h_{small}$$

Volume of big cylinder:

$$V_{big} := \pi r_{big}^2 h_{big}$$

Volume of pontoon:

$$V_{pont} := [\pi \cdot (r_{pont})^2 (L - d_{small})]$$

Volume of horizontal brace:

$$V_{hor} := \pi \cdot r_{brace}^2 \cdot L_{hor}$$

Volume of diagonal brace:

$$V_{diag} := \pi \cdot r_{brace}^2 \cdot L_{diag}$$

Total volume:

$$V_{tot} := 4V_{small} + V_{big} + 4V_{pont} + 4 \cdot V_{hor} + 4 \cdot V_{diag} \quad V_{tot} = 4.713 \times 10^3$$

Weight calculation:

Weight of small cylinder:

$$M_{small} := \pi \cdot [r_{small}^2 - (r_{small} - t_{cyl})^2] \cdot h_{small} \cdot \rho_{st}$$

Weight of the big cylinder:

$$M_{big} := \pi \cdot [r_{big}^2 - (r_{big} - t_{cyl})^2] \cdot h_{big} \cdot \rho_{st}$$

Weight of the pontoon:

$$M_{pont} := \pi \cdot [r_{pont}^2 - (r_{pont} - t_{pont})^2] \cdot (L - d_{small}) \cdot \rho_{st}$$



Weight of the horizontal brace:

$$M_{hor} := \pi \cdot [r_{brace}^2 - (r_{brace} - t_{brace})^2] \cdot L_{hor} \cdot \rho_{st}$$

Weight of the diagonal brace:

$$M_{diag} := \pi \cdot [r_{brace}^2 - (r_{brace} - t_{brace})^2] \cdot L_{diag} \cdot \rho_{st}$$

Total weight of the structure:

$$M_{tot} := 4M_{small} + M_{big} + 4 \cdot M_{pont} + 4 \cdot M_{hor} + 4 \cdot M_{diag}$$

$$M_{tot} = 8.518 \times 10^5$$

Corrected weight to compensate for local thickening:

$$M_{totcor} := M_{tot} \cdot 1.15$$

$$M_{totcor} = 9.796 \times 10^5$$

Buoyancy force calculation:

Buoyancy force:

$$F_b := \rho \cdot V_{tot} \cdot g$$

$$F_b = 4.739 \times 10^7$$

Reserve buoyancy force (Buoyancy force - weight structure - weight WT):

$$F_{b2} := F_b - (M_{totcor} + M_{wt}) \cdot g$$

$$F_{b2} = 2.993 \times 10^7$$

Buoyancy center calculation:

Cross sectional area small cylinder:

$$A_{small} := d_{small} \cdot h_{small}$$

Cross sectional area big cylinder:

$$A_{big} := d_{big} \cdot h_{big}$$

Cross sectional area pontoon:

$$A_{pont} := d_{pont} \cdot (L - d_{small})$$

Cross sectional area horizontal brace:

$$A_{hor} := d_{brace} \cdot L_{hor}$$

Cross sectional area diagonal brace:

$$A_{diag} := d_{brace} \cdot L_{diag}$$

Total cross sectional area:

$$A_{tot} := A_{small} \cdot 4 + A_{big} + A_{pont} \cdot 4 + A_{hor} \cdot 4 + A_{diag} \cdot 4$$

The height of the center of buoyancy calculated from the bottom:

$$y_{bc1} := \frac{A_{big} \frac{h_{big}}{2} + 4 \cdot A_{small} \frac{h_{small}}{2}}{A_{tot}}$$

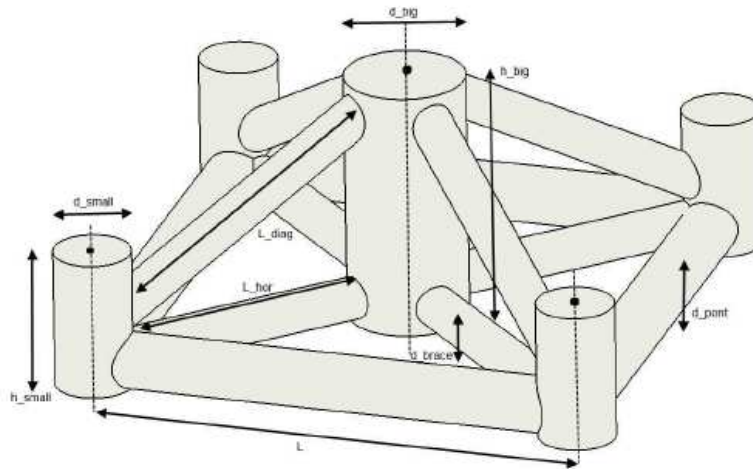
$$y_{bc2} := \frac{4A_{pont}r_{pont} + 4 \cdot A_{hor}r_{pont} + 4A_{diag} \left[\frac{(h_{big} - l - r_{pont})}{2} + r_{pont} \right]}{A_{tot}}$$

The height of the center of buoyancy for the top center coordinate system

$$y_{bc} := -h_{big} + (y_{bc1} + y_{bc2})$$

$$y_{bc} = -14.693$$

Figure of the TLP structure, with its design parameters given:





Appendix U Unused models and analyses

The previous chapters showed the used models and analyses which contributed to the improvement of the design. Beside these models, there were also models and analyses performed which did not work or were not useful. These will be discussed in this chapter.

Wave loading in Modal/PSD analysis

On the TLP structure wave current and hydrostatic loading also have to be applied. The impact of the waves and the ability to withstand this wave loading had to be analysed.

The conventional and commonly used method is doing a modal analysis to determine the behaviour of the structure in a transfer function. This transfer function will be used in combination with the spectrum of the waves. This will result in a response Power Spectrum Density. The response PSD can be used for the fatigue strength calculations of the structure due to wave loading.

This commonly used method was tried to use in Ansys. Unfortunately Ansys had limited options regarding this method and was not able to perform a good PSD analysis which represented waves loading. Therefore this common method could not be used for the fatigue strength analysis.

Modelling of wave loading in Pipe model

Since the commonly used method could not be done, other methods of analysing the response of the structure due to wave loading were investigated.

Ansys gives a special option for wave loading in a static analysis for certain element types; two of these element types are the used PIPE289 and LINK180 elements. The wave loading is applied with use of special OCxxx commands. With these commands an ocean environment can be described with different wave loading methods. The wave spectra could be specified easily with the use of the Pierson-Moskowitz spectra. Analyses with these commands were done.

However when analysing the results, they appeared to be unreliable. Several times a different result for the same settings was seen. The background information on the wave loading in Ansys was minimal and insufficient for the problem at hand. No possible solution for the problem could be found. It is unclear how the program calculates the behaviour of the structure, especially in a static analysis. This should be done in a similar way as the modal/PSD analysis described in the section above to get confident and reliable results. This does not seem to be the case for these wave load commands. Therefore this method is not used for wave loading.



Modelling of wave loading in Workbench

Similar to the wave loading of the Pipe model in APDL, wave loading was tried to be modelled in Workbench. This was also done with the Pipe and Link elements.

Although Workbench gives a better overview of the input and output, the results still showed alternating displacements for the same settings.

Although the results gave a little more insight on the behaviour of the structure, it was still not reliable to use for analysing the structure. It was still not clear how Ansys calculates the behaviour of the structure.

Possible use of FATjack and Beamcheck

Two possible applications provided by Ansys for the fatigue and ultimate strength assessment of the structure were checked for usability. These two applications are Fatjack and Beamcheck. The applications require the results obtained with the wave loading commands in Workbench.

Beside the fact that the results of the wave loading seemed to be unreliable, also the method how these programs did their strength assessment was unclear. This should be known, especially when certification is required. Therefore these applications were not used.